BERKELEY LAB

NUCLEAR SCIENCE DIVISION

Next Generation Gamma-Ray Spectrometers

Heather Crawford

Nuclear Science Division, Lawrence Berkeley National Laboratory

Topics

- **Lecture 1 – Gamma-Ray Detection Considerations**
  - Types of gamma-ray detectors – pros and cons, limitations
  - Evolution of spectrometers for nuclear structure & reactions
  - Resolving Power and Array Performance
- **Lecture 2 – Advanced Gamma-Ray Spectrometers and Nuclear Structure**
  - Gamma-ray tracking detector ingredients
  - The Gamma-Ray Energy Tracking Array (GRETA)
  - Physics beyond energies - angular distributions and linear polarization

Resolving Power and Array Performance

Optimized resolution, peak-to-total and efficiency **at the same time**

The science reach of a γ-ray tracking array can be expressed in terms of the effective resolving power (RP)

Depends on Efficiency (ε); Peak-to-Total (P/T); Resolution (δE)

Resolving Power = Science

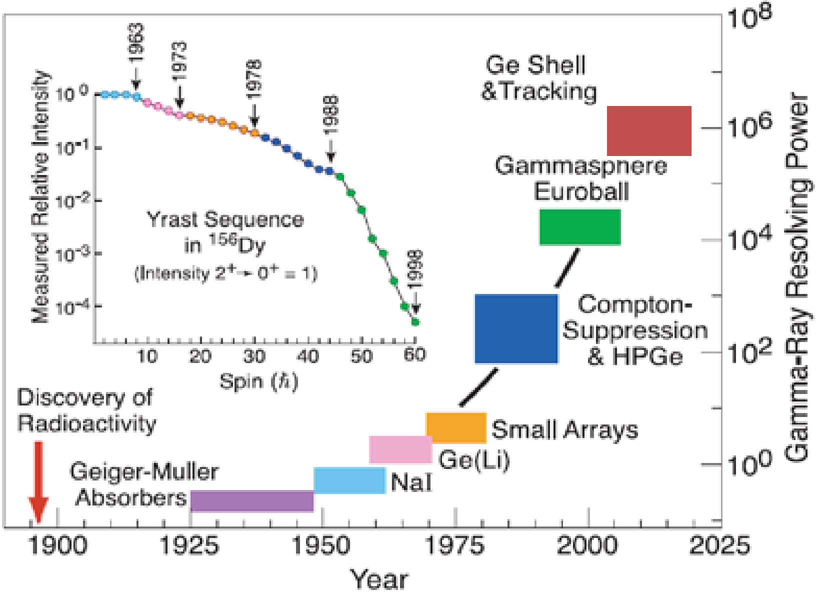

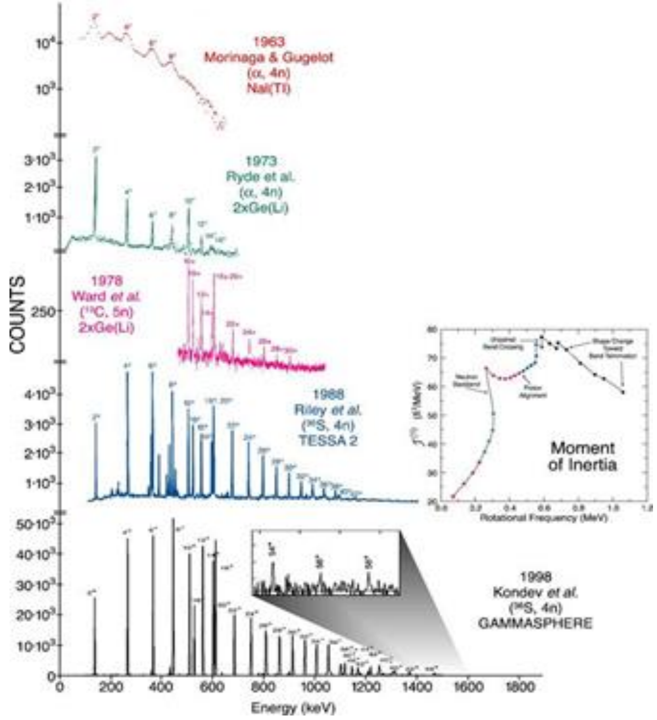

Compton Suppression and Gamma-Ray Tracking

Optimized resolution, peak-to-total and efficiency **at the same time**

Compton Suppressed Ge | Ge Sphere | Gamma Ray Tracking

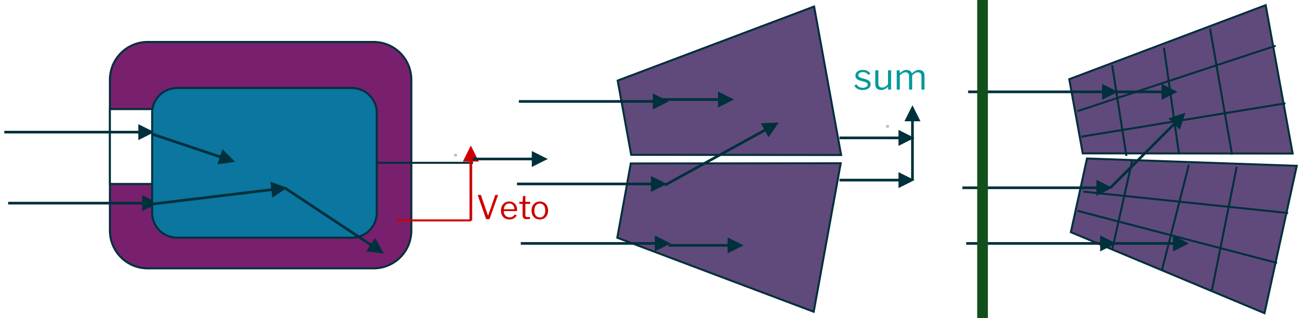

Compton Suppressed Ge	Ge Sphere	Gamma Ray Tracking
N = 100	N = 1000 (summing)	N = 100
NΩ e = 0.1	NΩ e = 0.6	NΩ e = 0.6
Efficiency limited	Too many detectors	Segmentation

Build a 4π sphere of Ge, using highly-segmented detectors
Gamma-ray tracking allows rejection of Compton scattering events,
Signal decomposition allows sub-segment position resolution

BERKELEY LAB

Gamma-Ray Energy Tracking Array Ingredients

https://greta.lbl.gov/community/workshops/trackingschool/schedule

Signal Decomposition

Remember R. Cooper's First Lecture Last Wednesday…

- Radiation interaction produces electron-hole pairs
- Charge cloud drifts to the electrodes under the influence of the applied electric field
- **As charges drift through the changing weighting potential, they induce a signal on the electrodes**

Laplace's equation

$$\nabla^2 V = 0$$

Signal Decomposition

Remember R. Cooper's First Lecture Last Wednesday…

The Weighting Potential of the neighbouring strip(s) extends into the 'hit' strip to give rise to image charges

Weighting Potential of a neigbour strip

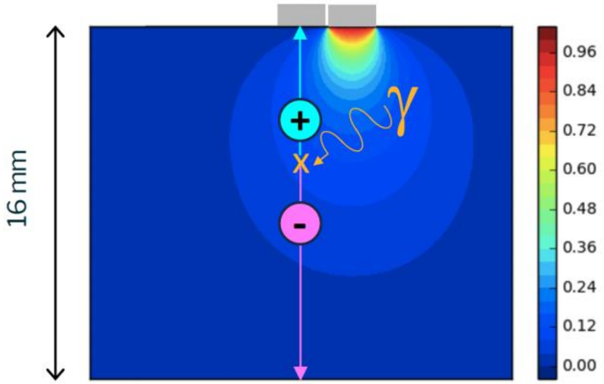

Signal

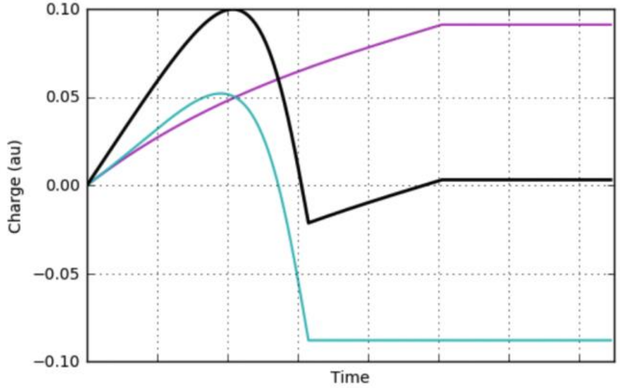

Signal Decomposition – **Electric Fields** and Weighting Potentials

- The electric field defines the motion of charge in the HPGe crystal (trajectory, drift velocity)
- To calculate the electric field, we compute the position-dependent electric potential by solving Poisson's equation

$$\nabla^2 V = -\frac{\rho}{\varepsilon}$$

$$\frac{d^2V}{dx^2} + \frac{d^2V}{dy^2} + \frac{d^2V}{dz^2} = -\frac{\rho}{\varepsilon}$$

- In practice, we do this using the relaxation method (a numerical method) – make an initial guess at V, respecting boundary conditions, update each 'pixel' based on neighbours and iterate until converged!

$$V'(x,y) = \frac{V(x+\delta,y)+V(x-\delta,y)+V(x,y+\delta)+V(x,y-\delta)}{4} + \frac{\rho(x,y)}{\varepsilon}$$

Signal Decomposition – **Electric Fields** and Weighting Potentials

Other initial ingredients:

- Impurity concentrations ⇒ depletion voltage
- Operating voltage

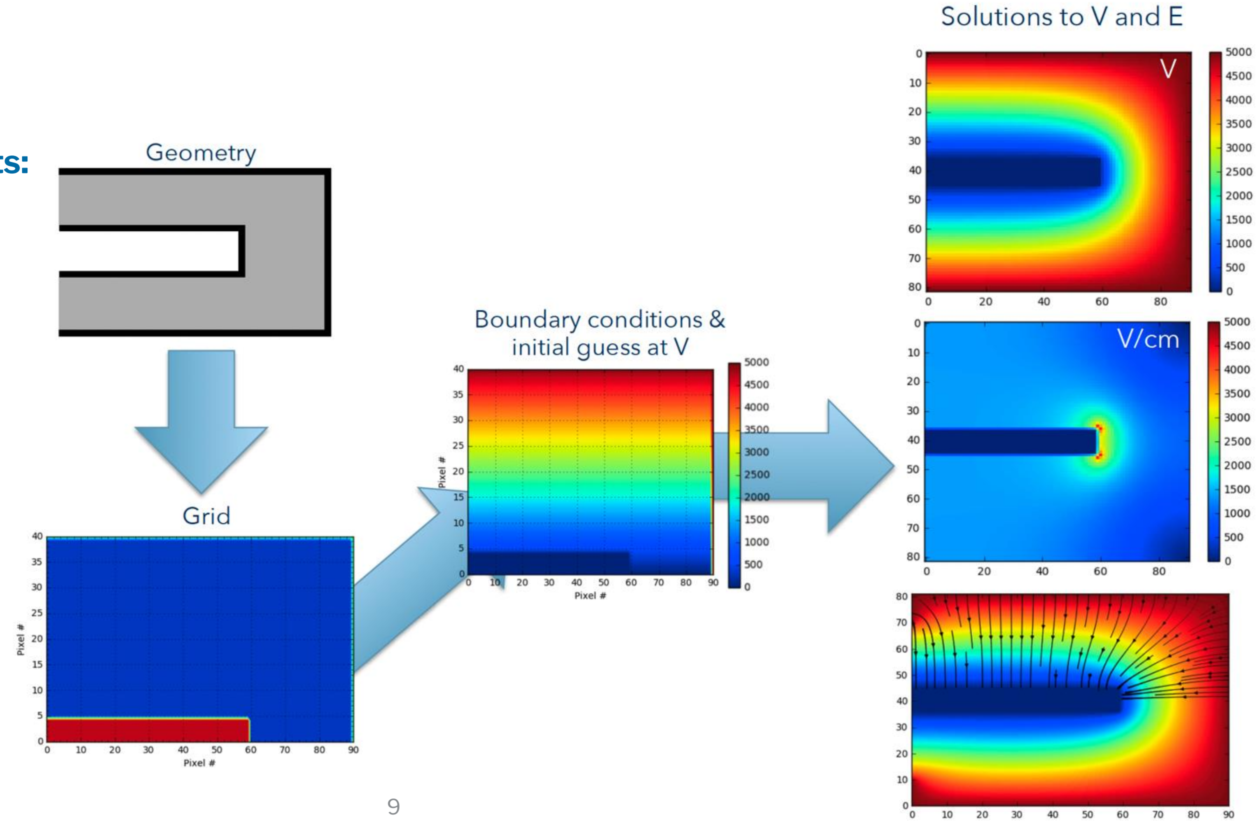

BERKELEY LAB

Signal Decomposition – Electric Fields and **Weighting Potentials**

- Weighting potential describes the (position-dependent) electrostatic coupling between an electrode and charge carrier
- Needed to calculate the signal induced on each electrode during the drift of charge carriers

- Charge induced on an electrode is given as:

Charge induced vs. time
i.e. the signal

hole charge

electron charge

$$Q(t) = +q\Delta W_h + -q\Delta W_e$$

Weighting fields experienced by
holes and electrons

Signal Decomposition – Electric Fields and **Weighting Potentials**

- Calculate weighting potential by solving the Laplace equation

$$\nabla^2 V = 0$$

- Boundary conditions – set electrode of interest V = 1 and all other electrodes to V=0
- Weighting potential depends on the geometry of the detector/electrodes

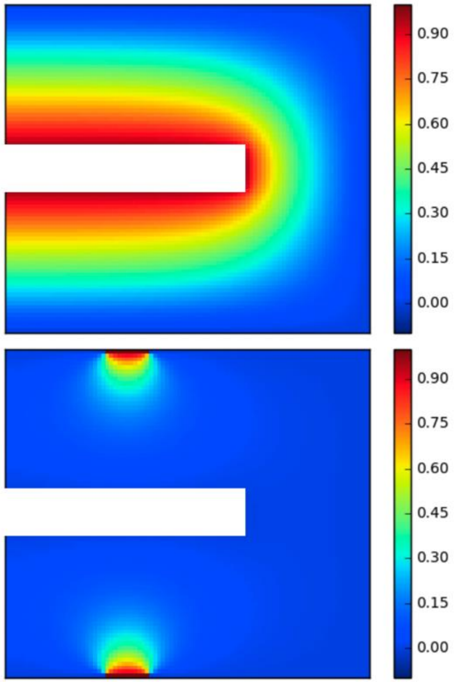

BERKELEY LAB

NUCLEAR SCIENCE DIVISION

Signal Decomposition – 'Pristine Basis' Calculation

- With the electric field and weighting potentials calculated can calculated the set of signals for a point charge 'dropped' in the detector at any position
- Only additional information needed is the drift velocity of the charge carriers (relates to temperature and crystal axis orientation)
- Calculate signals for ~250,000 points in each GRETA crystal, on an irregular grid in which points are equidistant in sensitivity (χ^2 difference between neighbouring points)

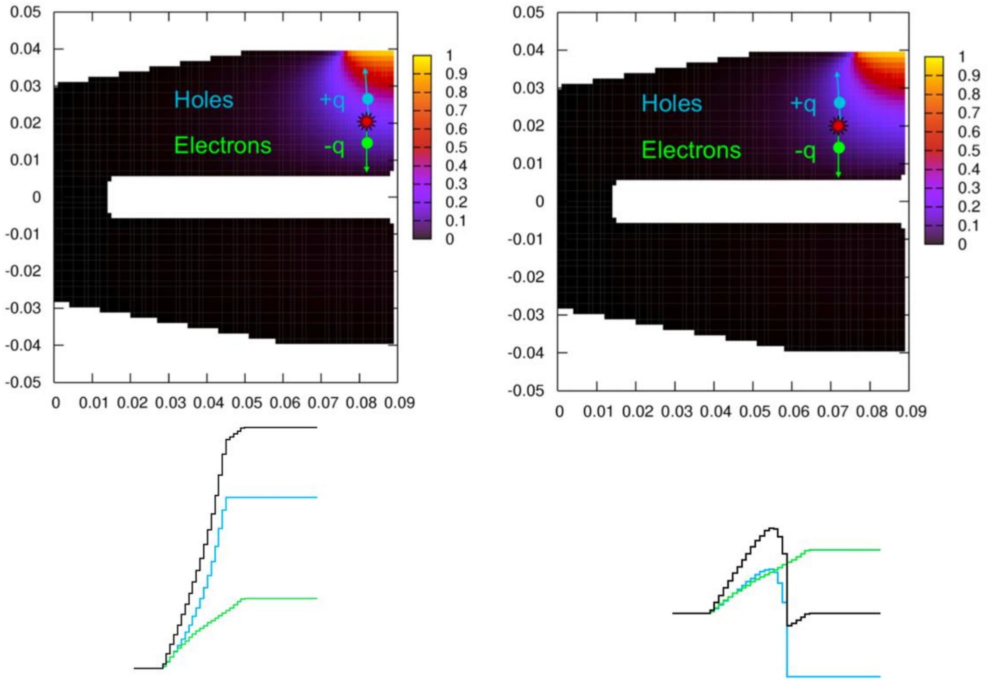

Signal Decomposition – 'Superpulse' Electronics Response

- Life is always more complicated…
- The electronics for all detector signals are closely packed together and cannot be fully isolated
- Differential cross-talk results in the derivative of a net-charge segment being imposed on neighbouring segments – this is **similar in magnitude** to induced signals
- We **must account for electronics response to have position sensitivity**

- Include 669 response parameters:
  - Preamplifier shaping times (segments, CC)
  - Differential cross-talk
  - Integral cross-talk
  - Time offsets between segments

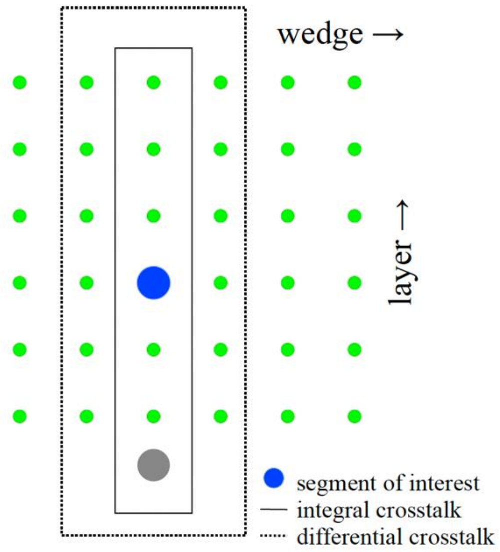

Signal Decomposition – ‘Superpulse’ Electronics Response

- Superpulse method – superpulses are a concatenation of 36 traces + CC
- Data are taken by selecting segment multiplicity = 1 events, with the full photopeak (^{60}Co) energy recorded in the single hit segment
- The same can be simulated based on GEANT4 and then signals calculated and averaged to create a calculated superpulse
- Why average waveforms?
  - Electronics response is independent of interaction point location in segment
  - Averaging reduces statistical fluctuations, enables fast data-taking
  - Washes out position dependent effects, removing some sensitivity to simulation

Signal Decomposition – ‘Superpulse’ Electronics Response

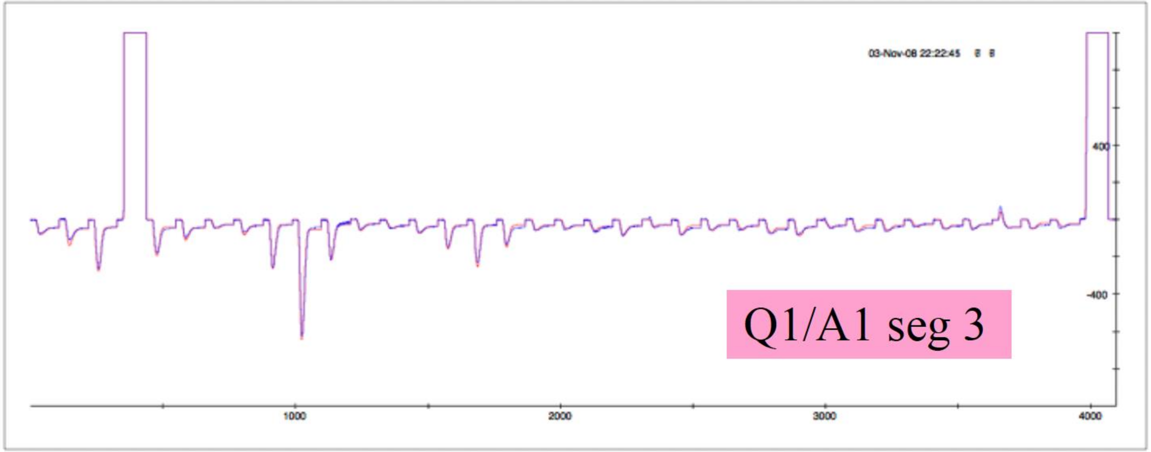

- With measured superpulse and calculated superpulse, fit parameters of the response function until the **corrected** calculated superpulse matches the measurement
- The same response parameters can then be applied to the points of the pristine basis to create the cross-talk corrected final basis for use in experiments

Signal Decomposition Algorithm (GRETA)

- GRETA uses adaptive grid-search fitting for signal decomposition
- Searched for **one hit segment** at a time – starting on a coarse grid (ever second basis point)
- Loop over all pairs of positions – we are looking for two hits
- Once the best pair is found based on χ^2, search on the finer (complete) grid for a better solution
- Non-linear least-squares is then used to interpolate between grid positions
- With two-interaction point solution, try adding a third point if χ^2 is bad (add with 1/3 of energy in the center of the segment)
- Try coalescing two interactions into one if closely spaced
- Select best overall with a penalty factor for extra interactions

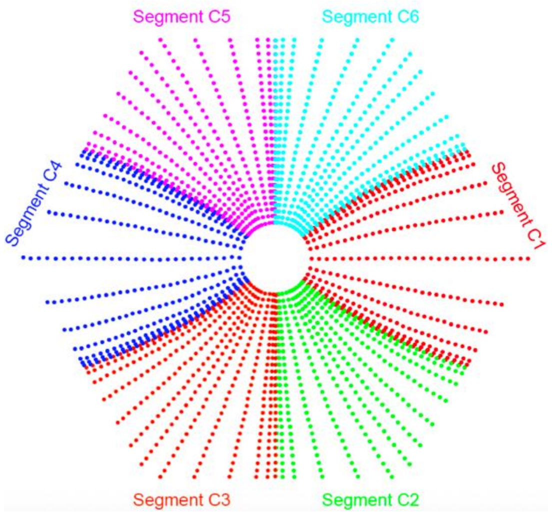

Signal Decomposition Algorithm (GRETA)

- **Multiple hit segments**
- Start by performing non-linear least squares to find one interaction per segment
- Subtract calculated signals for lower energy net segments from the maximum energy segment and then revisit the maximum energy net segment looking for pairs of interaction points
- Repeat for other segments to get pairs of interactions in all segments
- Evaluate possibility to coalesce interaction points (no more adding a third interaction point)

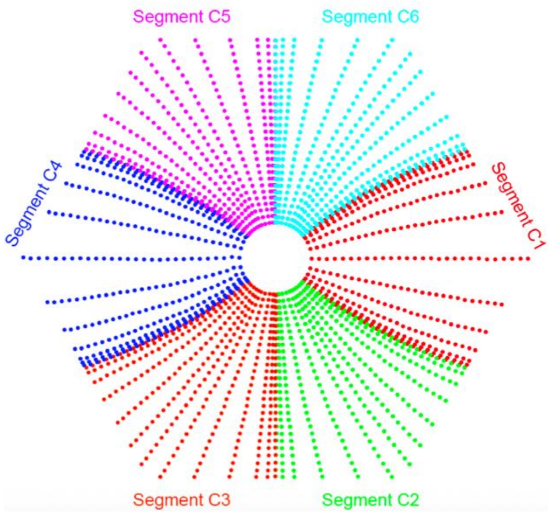

Signal Decomposition in GRETA

Induced charges constrain positions to ~mm^3

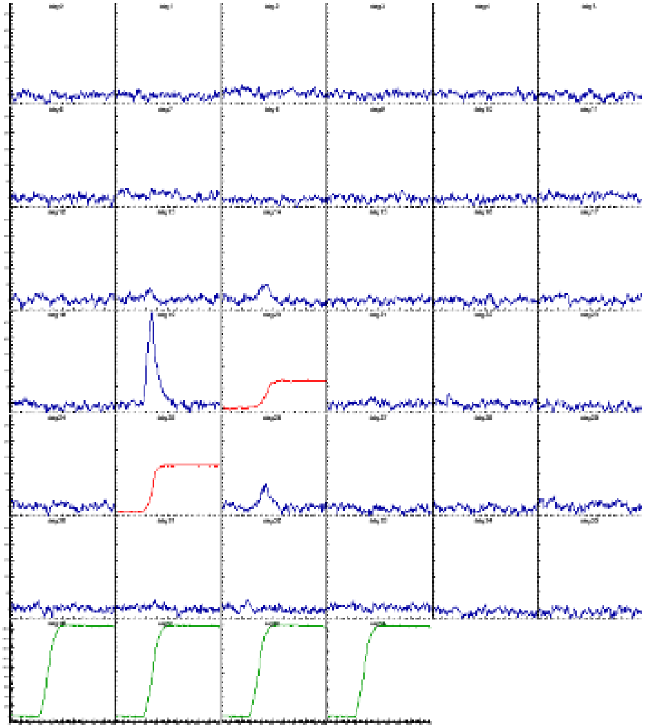

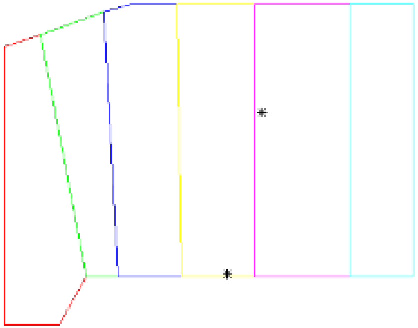

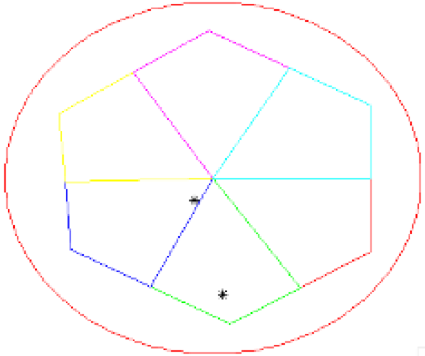

Gamma-Ray Tracking

Cluster interactions to recover the experimental event(s) as best as possible

- Data are interaction positions and energies – goal is to find ordered clusters of interactions that optimize a Figure of Merit
- First step is the clustering of points into likely scattering sequences – based on a cone opening angle (e.g. if angle between points θ is less than some threshold angle α)

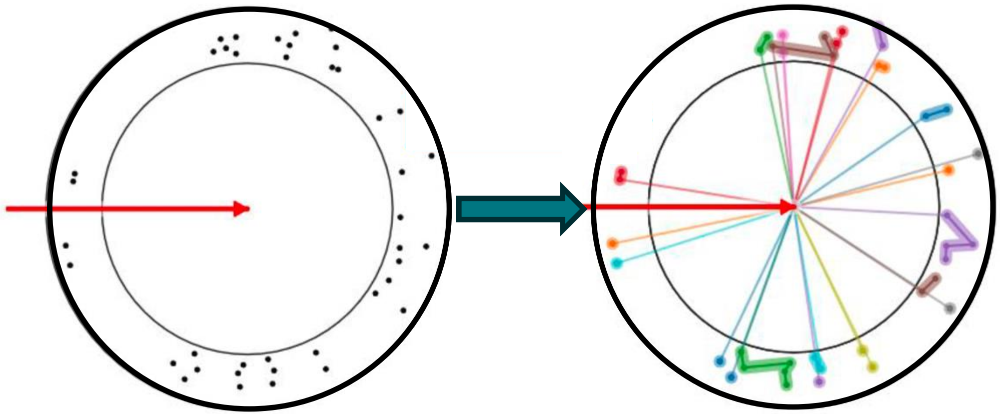

BERKELEY LAB

NUCLEAR SCIENCE DIVISION

Gamma-Ray Tracking: Figure of Merit

- Start with the assumption that the cluster contains the total energy of the gamma-ray, and that it originates from the target position
- Exhaustive tracking evaluates a FOM for all permutations of the interaction points

- Assumption is that if **energy is missing**, or if the **origin is not the target**, that even the best FOM will be poor

$$\mathrm{FOM} = \frac{1}{N-1}\sum_{i=1}^{N-1}\left(\theta^{geo} - \theta^{theo}(E_{i-1}, E_i)\right)^2$$

GRETINA (AFT) FOM

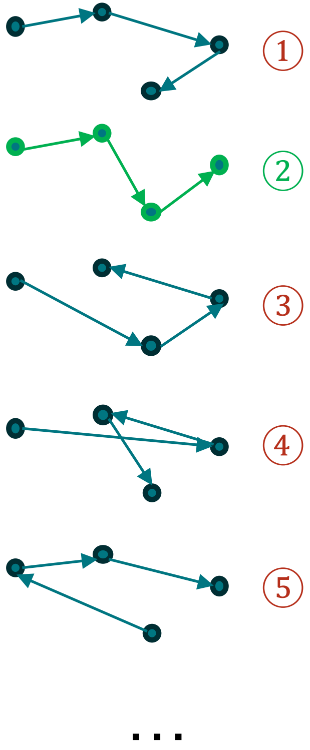

Gamma-Ray Tracking: FOM Cuts

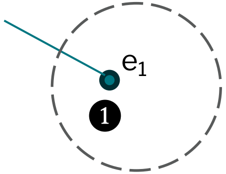

Single interaction
photo-electric effect
⇒ no FOM

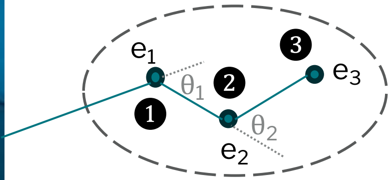

Compton scattering
⇒ ideal case

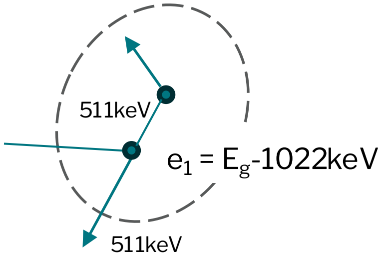

Pair production ⇒
special case, no good
single order of
interaction points

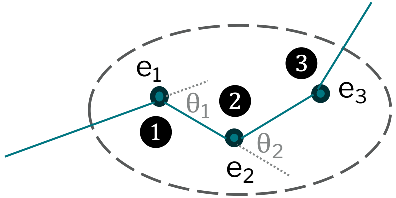

Escaped Compton
scattering ⇒ **should
have poor FOM**

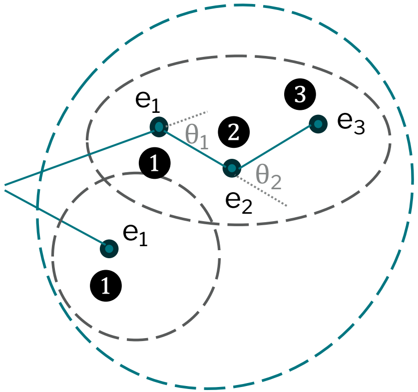

Combined gammas
in clustering ⇒ poor
FOM

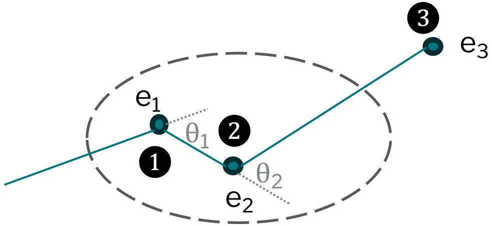

Clustering missed an
interaction point ⇒
poor FOM

Gamma-Ray Energy Tracking Array (GRETA)

Gamma-Ray Energy Tracking Array (GRETA)

The U.S. tracking array (cf. AGATA in Europe)

- GRETA uses large-volume highly segmented HPGe detectors to completely tile the sphere surrounding a target location (covering 80% of solid angle)
- Crystal segmentation and digital electronics enables localization of gamma-ray interaction points with ~mm^3 resolution
- With localized interaction points, gamma-ray tracking enables background rejection → P/T of Compton suppressed array

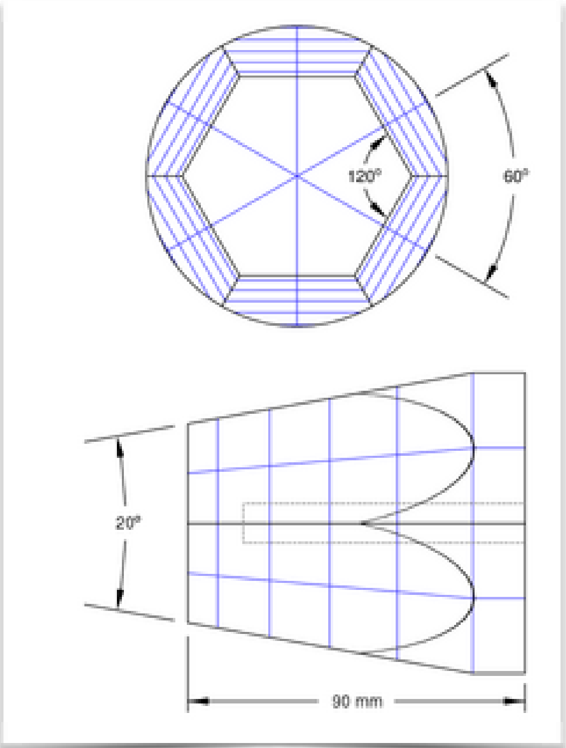

Integrating the Subsystems of GRETA

Detector Systems

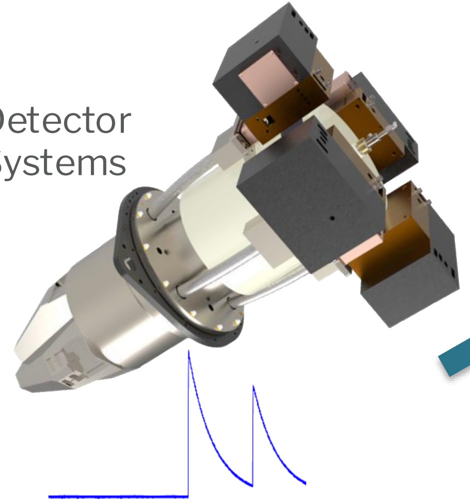

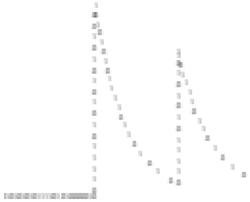

- Continuous 100MHz digitization of 40 preamplifier signals per crystal

Electronics Systems

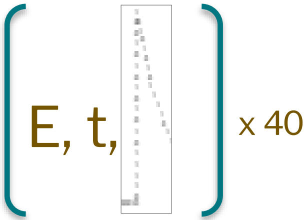

- FPGA-based energy filters, event selection in response to physics triggers

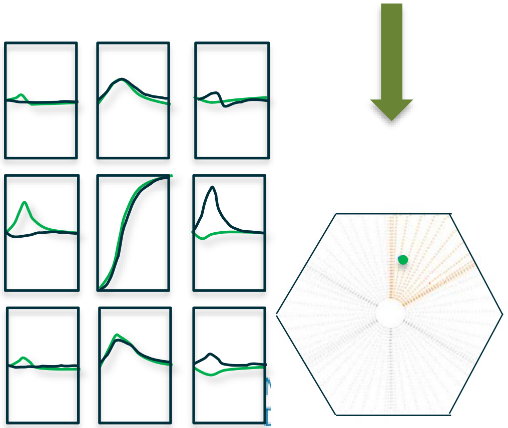

Integrating the Subsystems of GRETA

Detector Systems

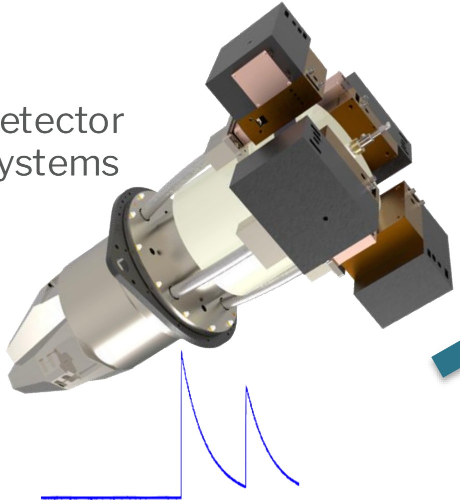

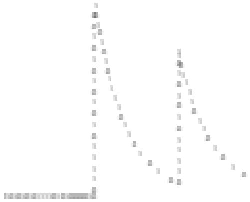

- Continuous 100MHz digitization of 40 preamplifier signals per crystal

Electronics Systems

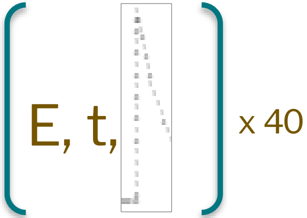

- FPGA-based energy filters, event selection in response to physics triggers

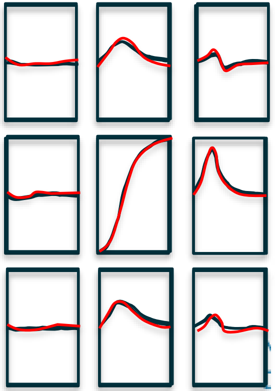

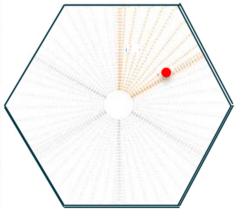

BERKELEY LAB

Integrating the Subsystems of GRETA

Detector Systems

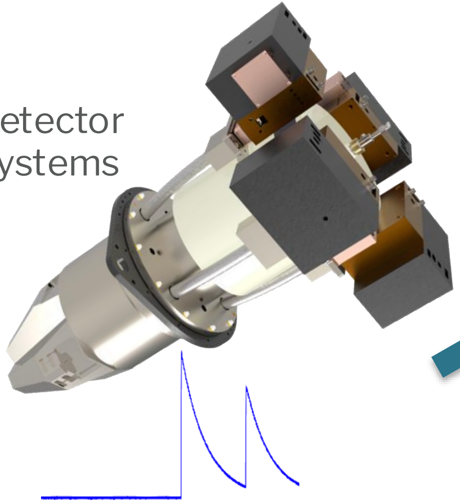

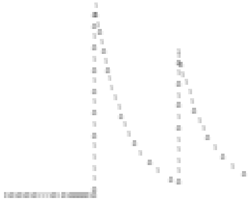

- Continuous 100MHz digitization of 40 preamplifier signals per crystal

Electronics Systems

E, t, 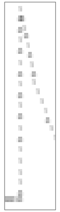 x 40

- FPGA-based energy filters, event selection in response to physics triggers

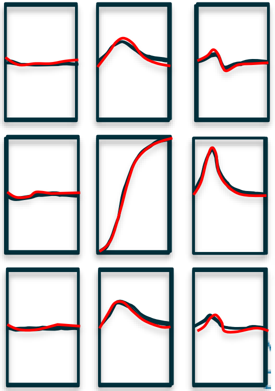

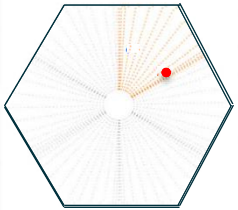

Computing Systems

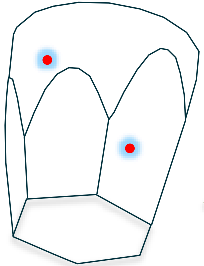

$$\left[E, t, (x, y, z)_{crystal}\right]_n$$

BERKELEY LAB

Integrating the Subsystems of GRETA

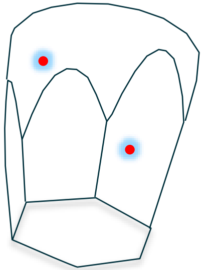

$$\left[E, t, (x, y, z)_{crystal}\right]_n$$

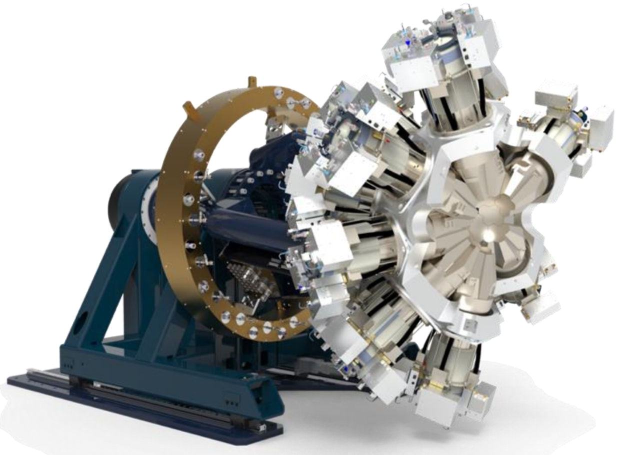

Mechanical Systems

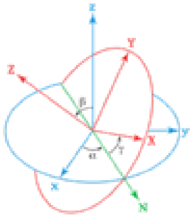

- Detectors located absolutely in space to +/- 0.4 mm

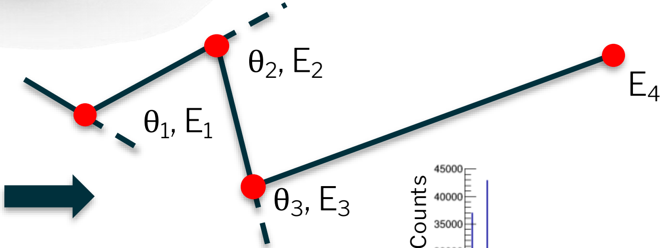

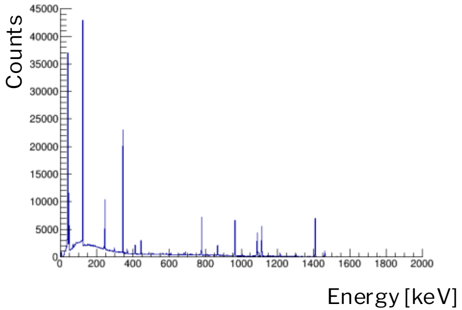

Compton Suppression and Gamma-Ray Tracking

Optimized resolution, peak-to-total and efficiency **at the same time**

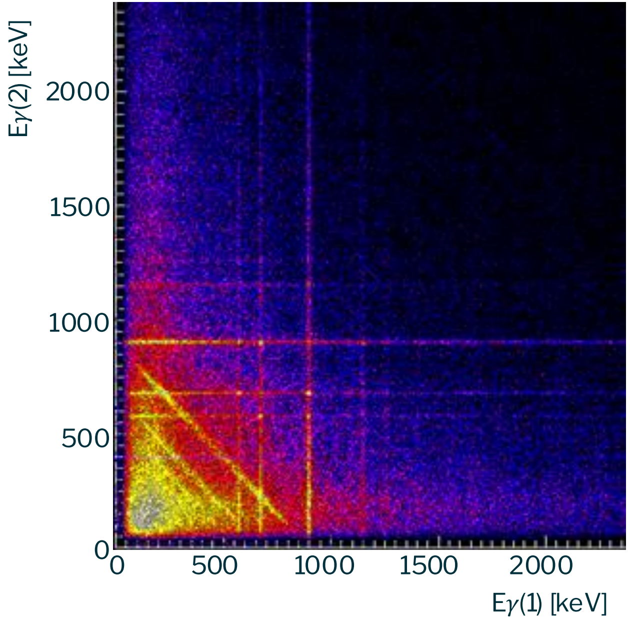

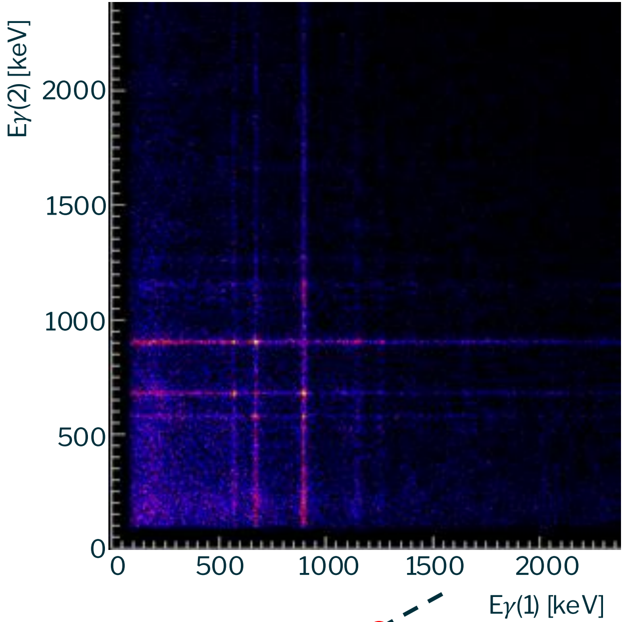

^{64}Ge populated in knockout from ^{65}Ge

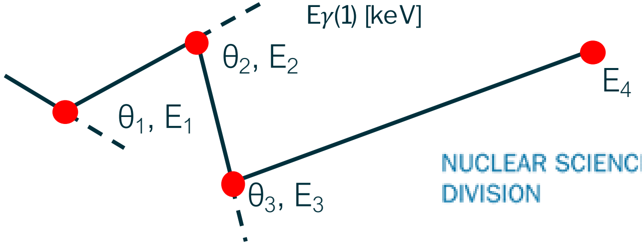

Reduction of Compton background by tracking allows spectral quality comparable to arrays with anti-Compton shields.

NUCLEAR SCIENCE DIVISION

GRETA Quad Detector Modules

23 Quads in Gamma Lab at FRIB

- The GRETA Quad detectors are identical to the modules used in GRETINA (operating since 2011)
- Quads were developed by LBNL in collaboration with Canberra/MIRION in the early 2000s
- Demonstrated performance and serviceability; experts within the GRETA project at FRIB and LBNL
- GRETA includes 18 (+1) Quads – **all** 19 are now delivered and accepted

GRETA Quad Detector Modules

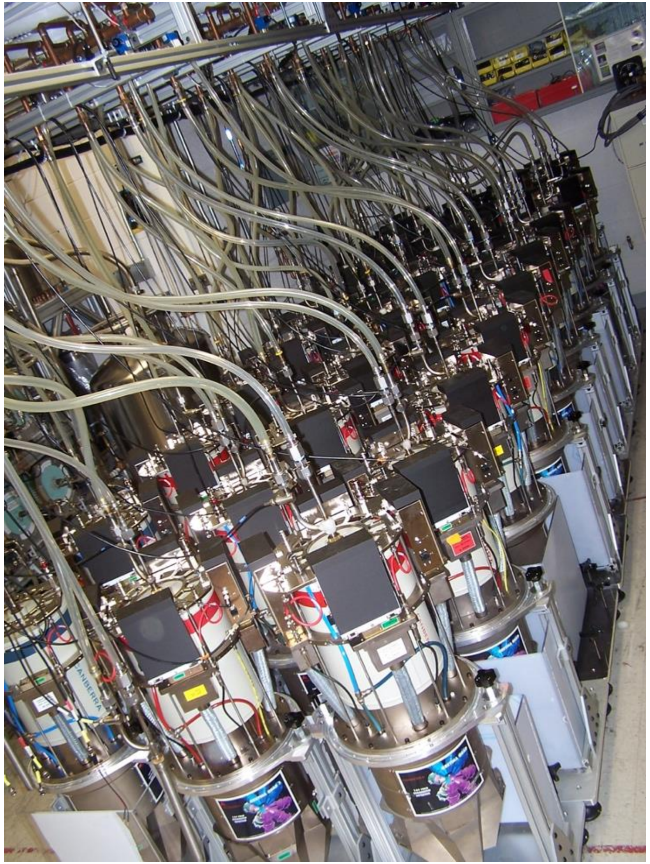

30+ Quads in Gamma Lab at FRIB

Electronics Systems

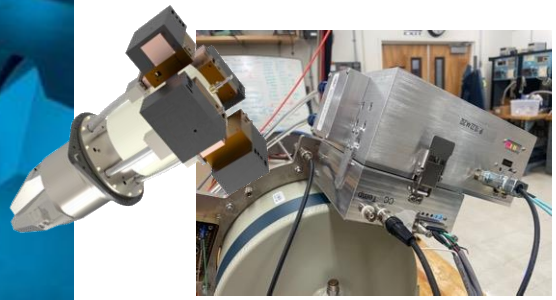

Electronics (ADC) are on the Detectors, Digitized signals sent to Signal Filter Boards

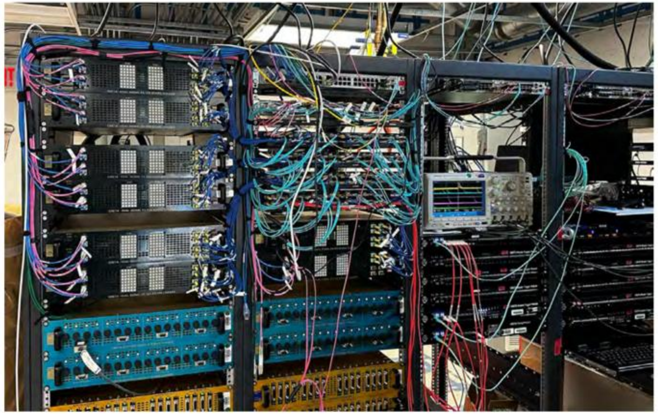

Digitize at the detector, fiber-based network carries data and controls

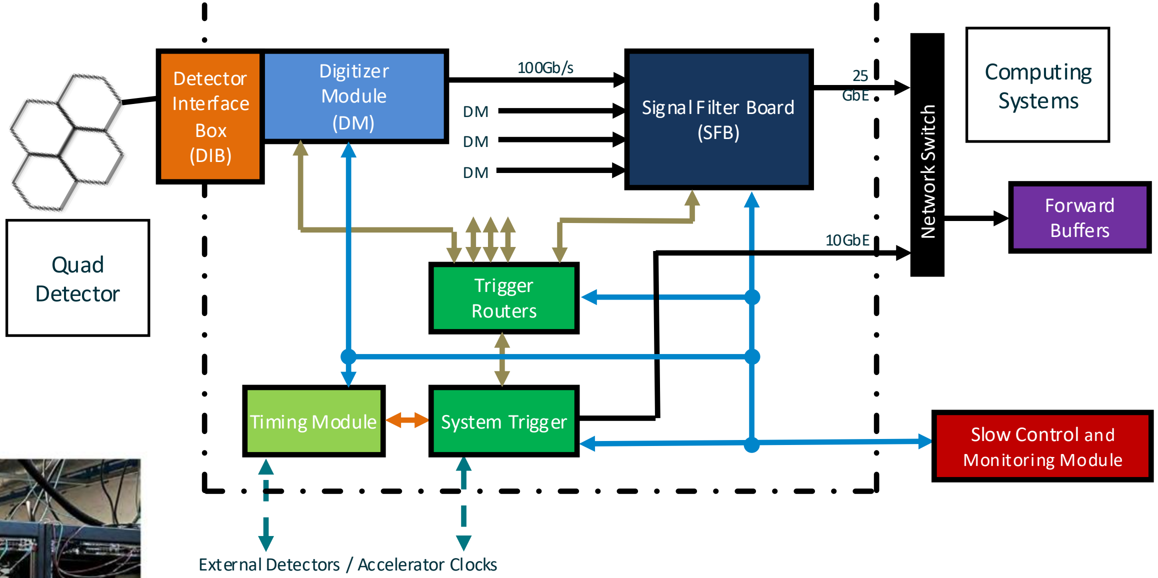

4800 Channels

- 120 Detector Interface Boxes and Digitizer Modules (DM)
- 16 Signal filter boards, 11 Trigger and Timing modules
- Ancillary systems (8 DM power supplies, 8 cable-break-out chassis, and associated signal and power cables/fibers)
- FPGA firmware

Electronics Performance – Linearity and Gain Stability

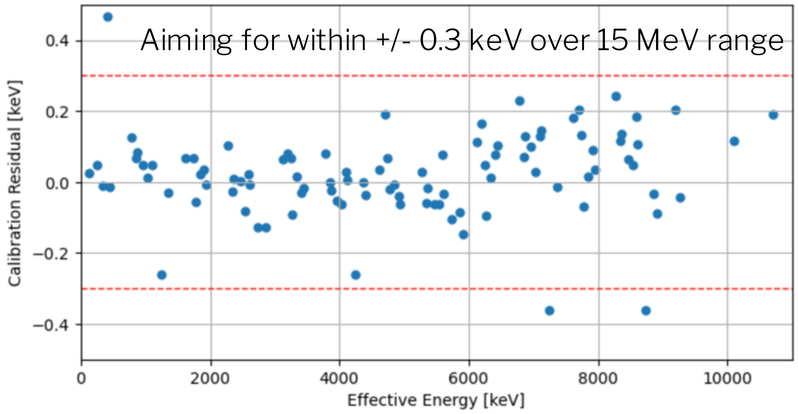

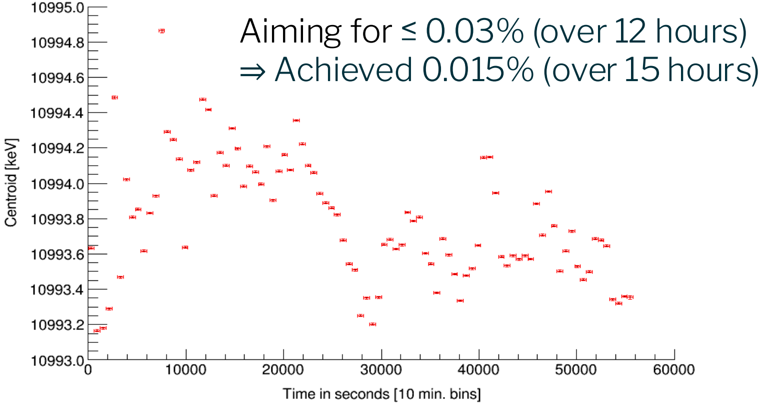

- The electronics performance was verified with testing across the duration of the project
- The digitizer is an extremely performant module, and detector mounted
- All power delivery met and exceeded the noise requirements
- The GRETA production systems delivery performance at the same level as fully optimized bench testing

Computing Systems

Pipeline-Based Network Architecture Enables Cutting-Edge Performance

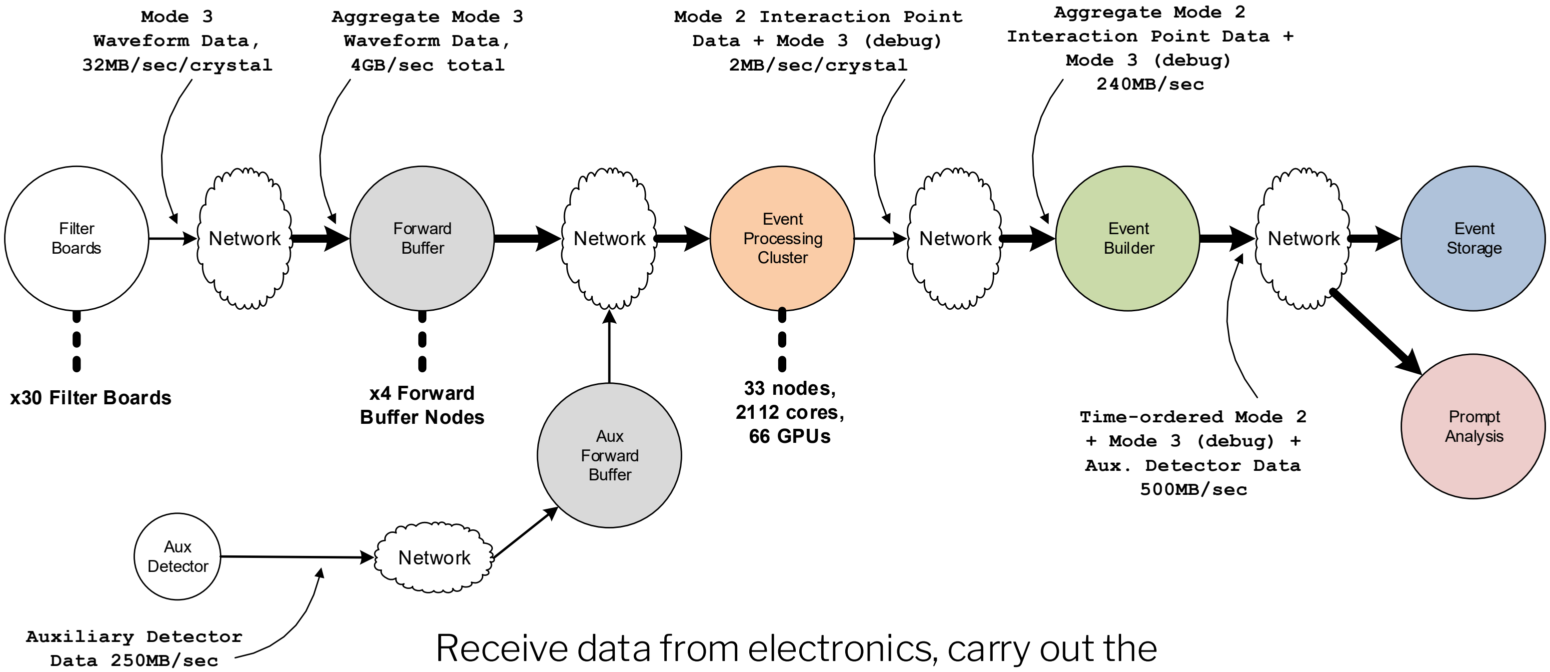

Receive data from electronics, carry out the signal decomposition calculations, and build events to store

Computing Systems

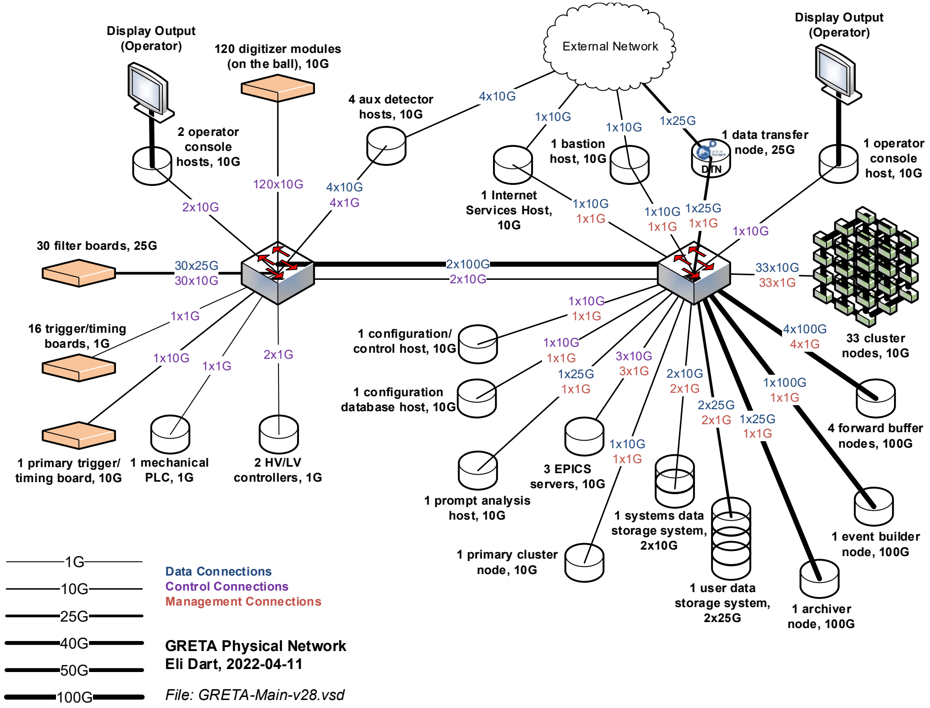

- With strong collaboration from ESnet, the GRETA computing team developed a novel pipeline-based network architecture to enable cutting edge performance
- High-performance computing cluster enables in-line compression and supports > 500k signal decomposition calculations per second
- 500TB full SSD storage improves ability to sort online, and move data quickly off the cache to the DTN

BERKELEY LAB

Mechanical Systems

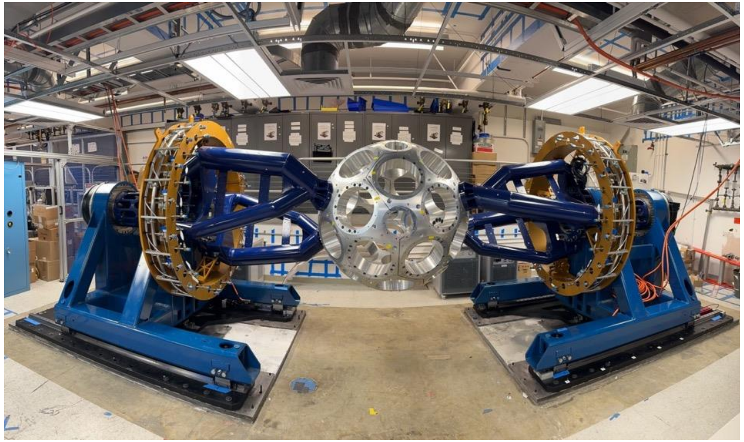

- 2 hemispheres each with 15 ports to locate a total of 30 Quad Modules (QDM)
- Achieved a position of QDM ≤ ±0.40 mm (x, y, z) as required
- Linear translation of 500 mm and rotation of +180 and -172 degrees meets the requirement to install all detectors from either side

Gap between adjacent QDM end-caps mounted in the array was measured to be 0.89 mm – 1.09 mm (1 mm nominal gap).

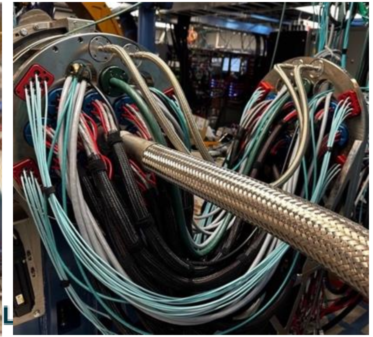

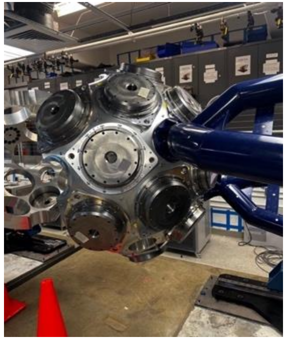

Hemispheres Fabrication Steps


Raw Material


First Inner Machining Step


First Rough Hemisphere


Ready for Last Machining Step


Ports Added to Hemisphere

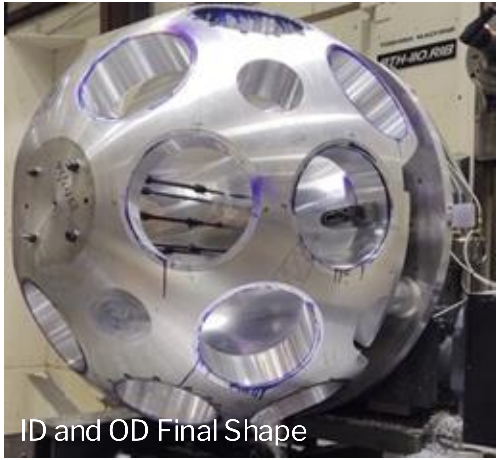
ID and OD Final Shape

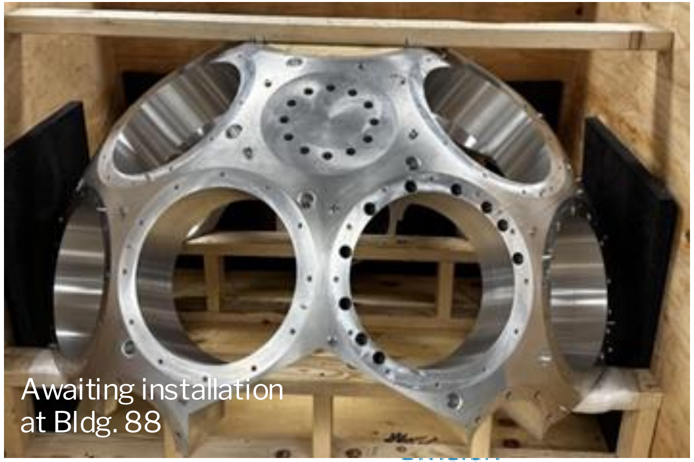
Awaiting installation at Bldg. 88

GRETA Performance

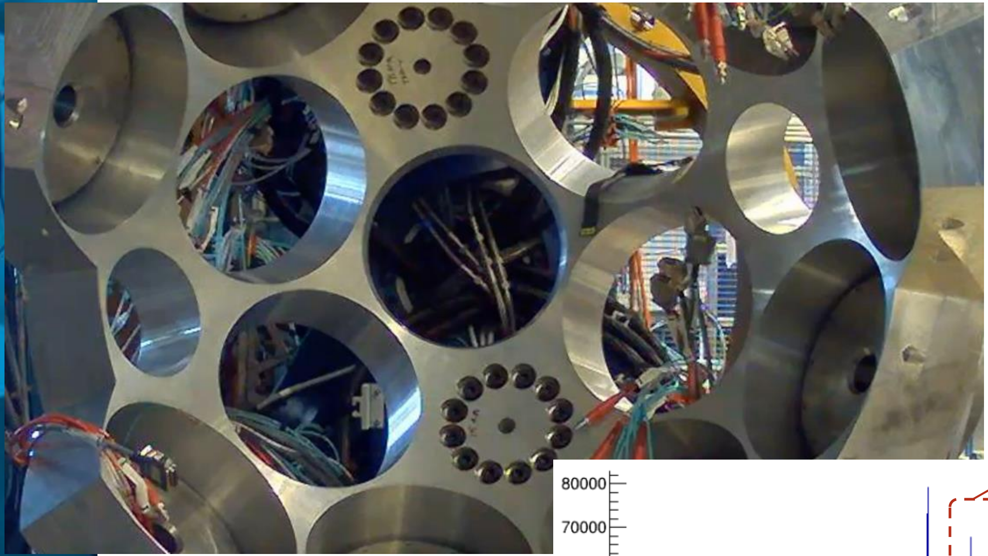

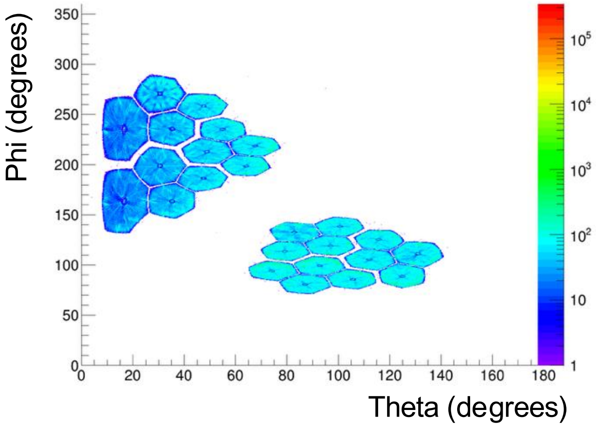

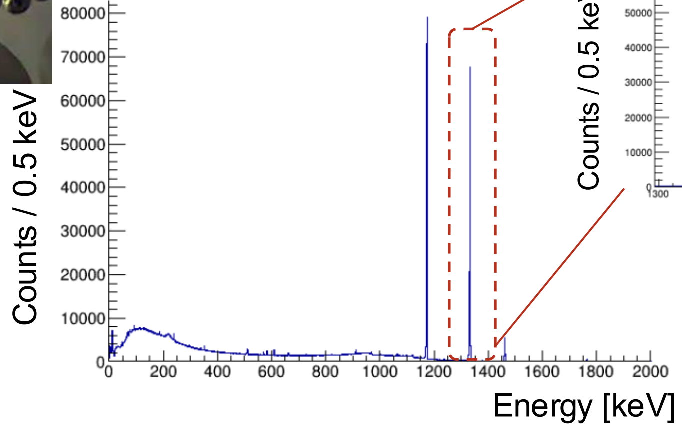

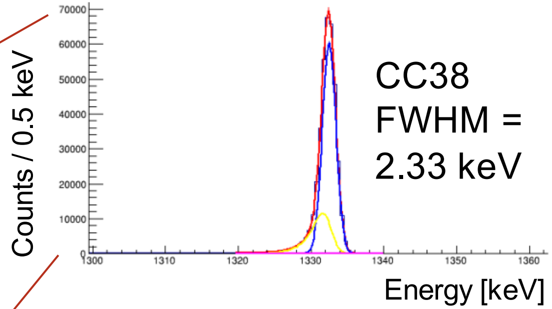

BERKELEY LAB

NUCLEAR SCIENCE
DIVISION

GRETA is Now at FRIB

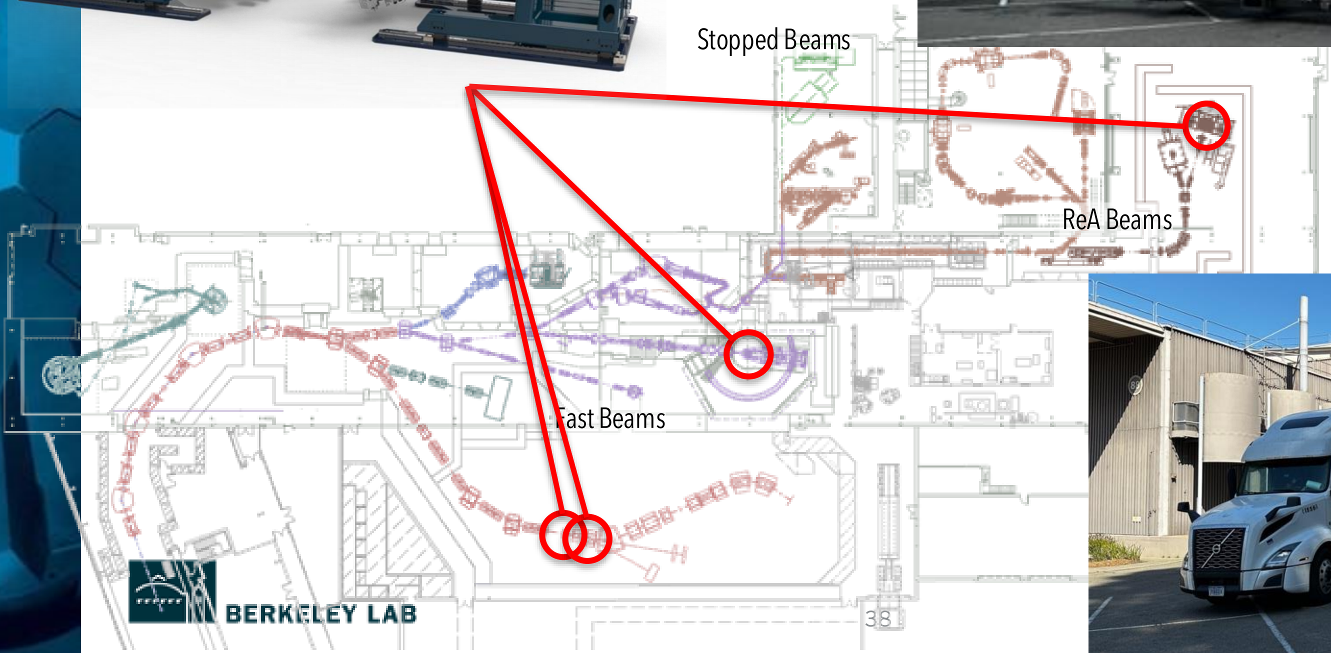

BERKELEY LAB

Installation at FRIB

- Installation at FRIB of the support frame, electronics and computing hardware was completed last Fall; the full complement of Quad modules was installed in the array over the last several months

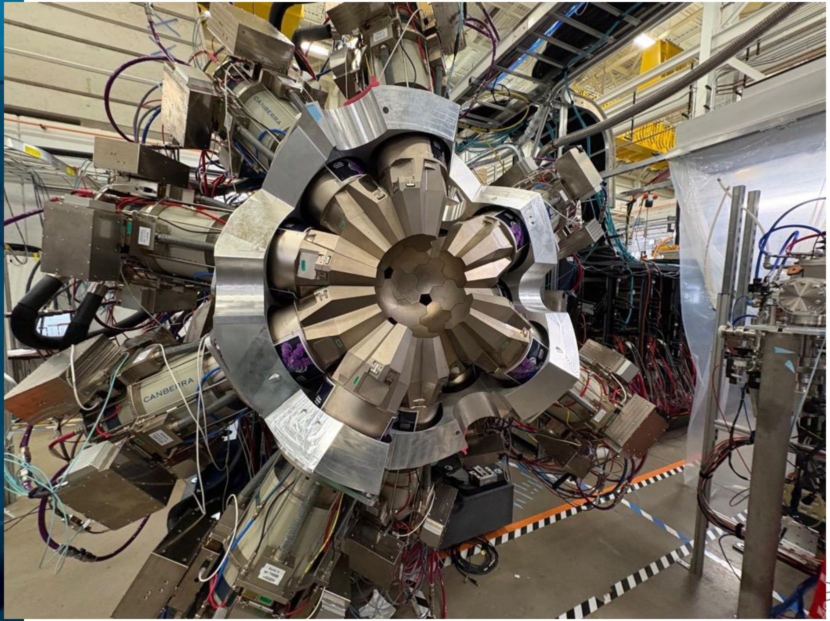

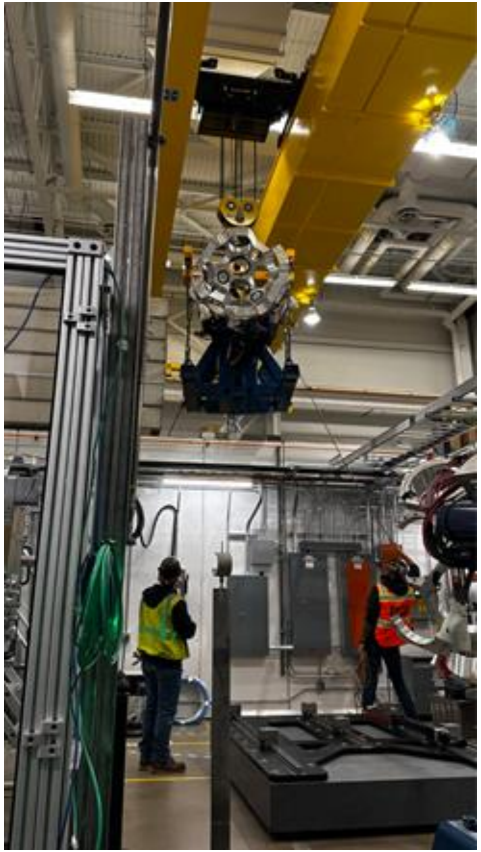

^{158}Er GRETA@ReA6

Fold 7 gated matrix   178 MeV ^{40}Ar + ^{122}Sn (0.5mg)   ~5*10^{8} pps (~33hrs data); 'online', not tracked

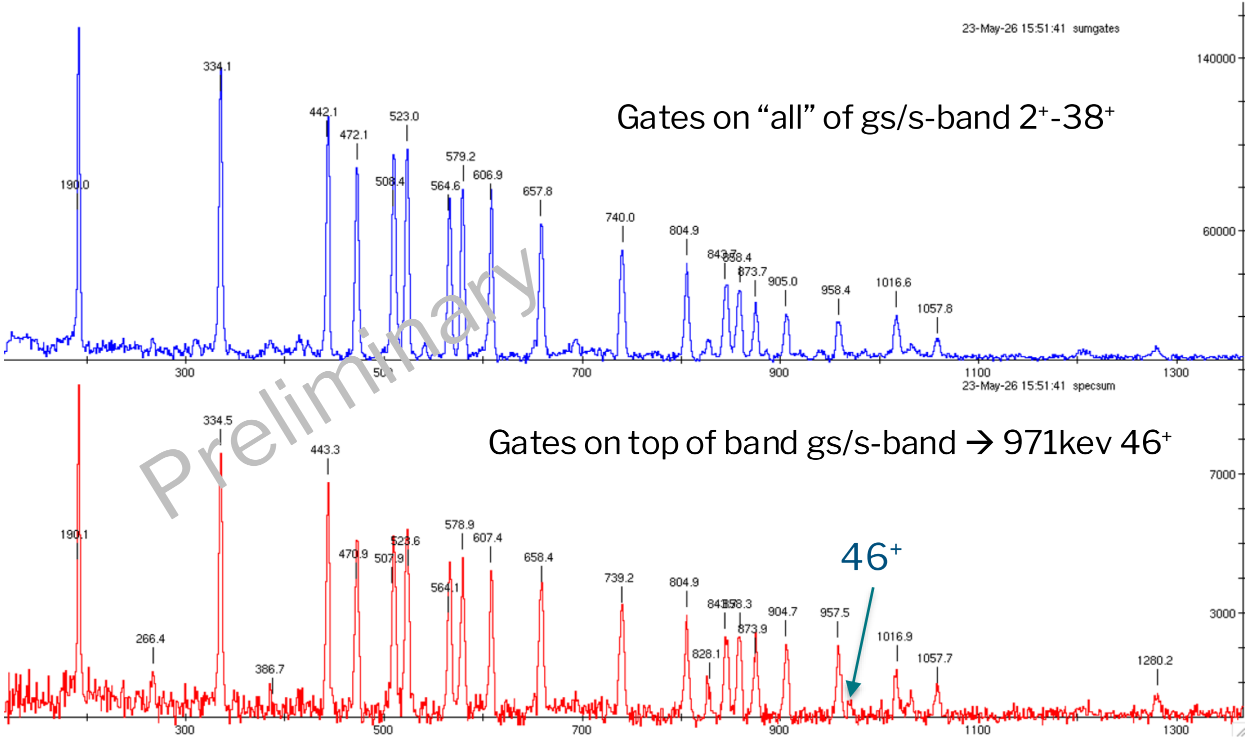

BERKELEY LAB

NUCLEAR SCIENCE DIVISION

^{158}Er GRETA@ReA6

Fold 7 gated matrix   178 MeV ^{40}Ar + ^{122}Sn (0.5mg)
~5*10^8 pps (~33hrs data); 'online', not tracked

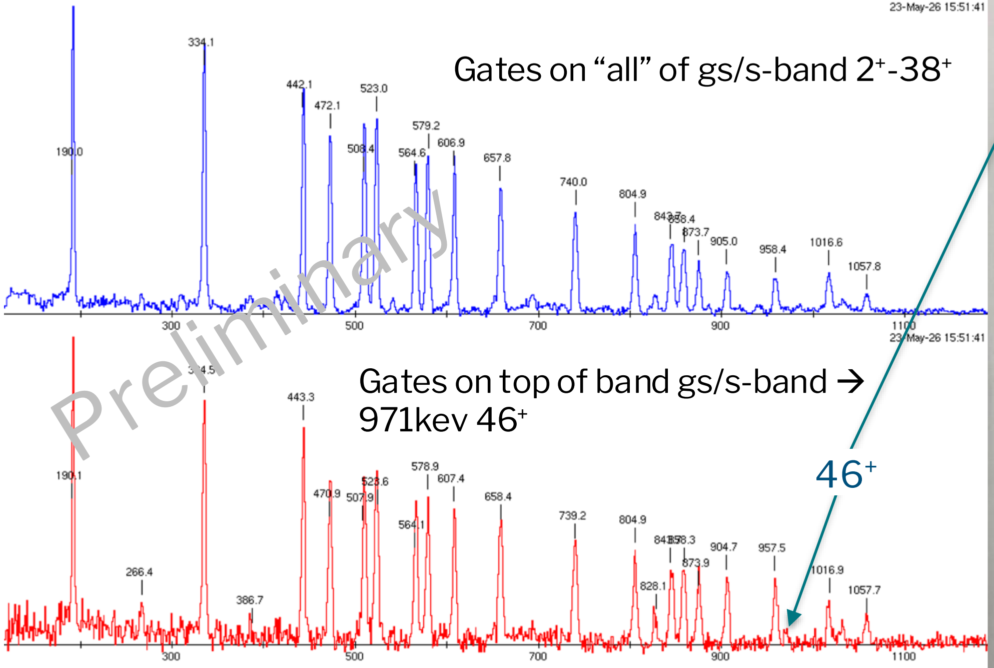

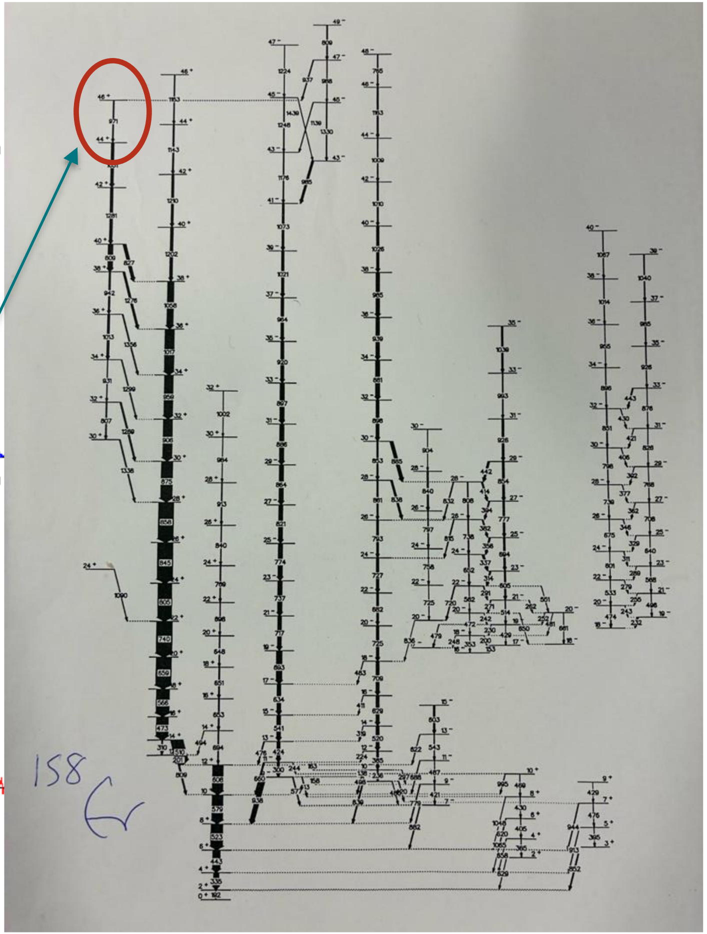

(A Very Little Bit of)
Physics with Tracking Arrays

Lifetimes from Peak Shapes

- The recoil distance method took advantage of differences in the recoil velocity after passing through degraders, and the incorrect Doppler correction which splits the measured transition
- Even without a degrader, an imperfect Doppler correction can be caused by an excited state lifetime – distorted lineshape

$T_{1/2}(4^+) = 4.7(6)$ ps

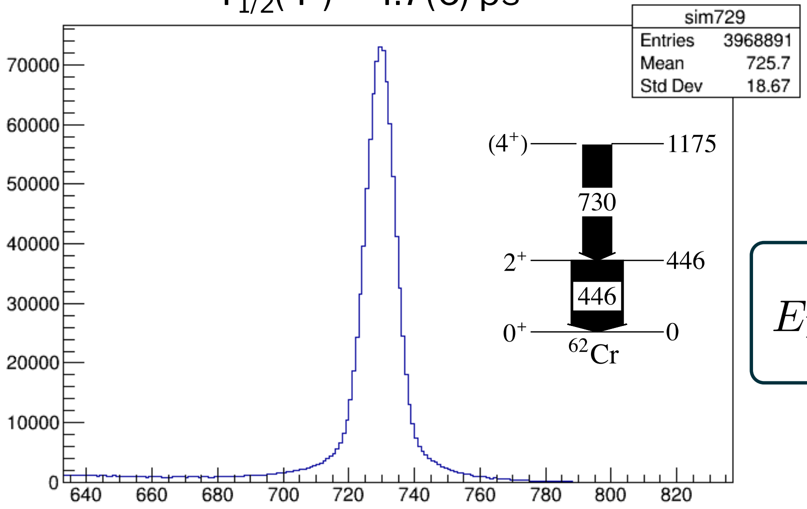

$$E_{\mathrm{lab}} = \frac{\sqrt{1-\beta^2}}{1-\beta\cos\theta} E_{\mathrm{cm}}$$

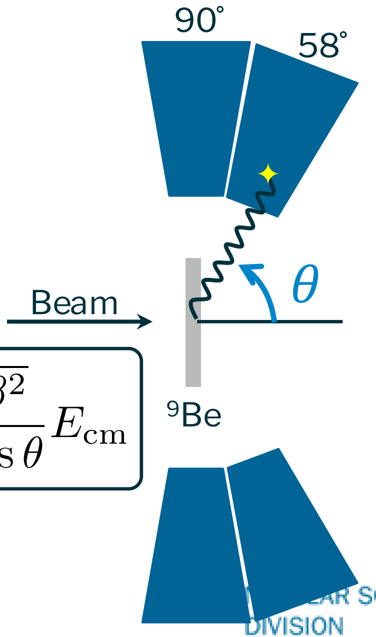

Lifetimes from Peak Shapes

- The recoil distance method took advantage of differences in the recoil velocity after passing through degraders, and the incorrect Doppler correction which splits the measured transition
- Even without a degrader, an imperfect Doppler correction can be caused by an excited state lifetime – distorted lineshape

$T_{1/2}(2^+) = 87(9)$ ps

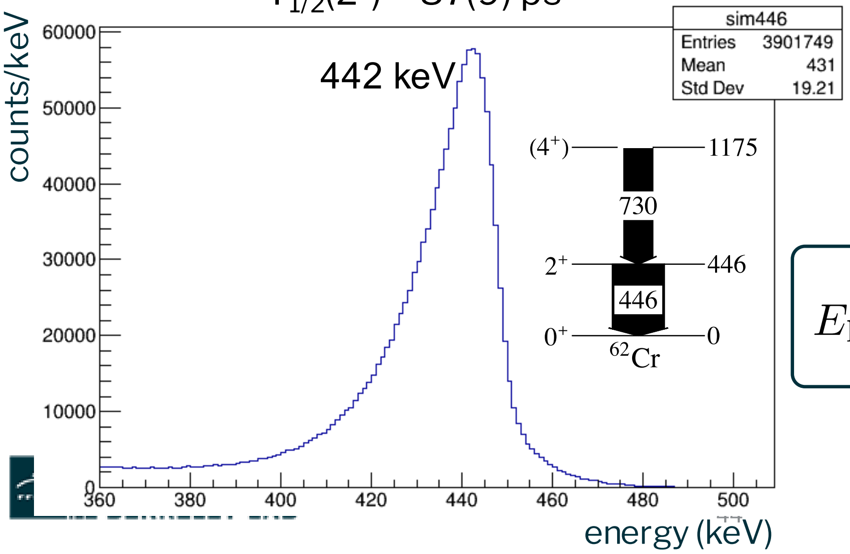

$$E_{\mathrm{lab}} = \frac{\sqrt{1-\beta^2}}{1-\beta\cos\theta} E_{\mathrm{cm}}$$

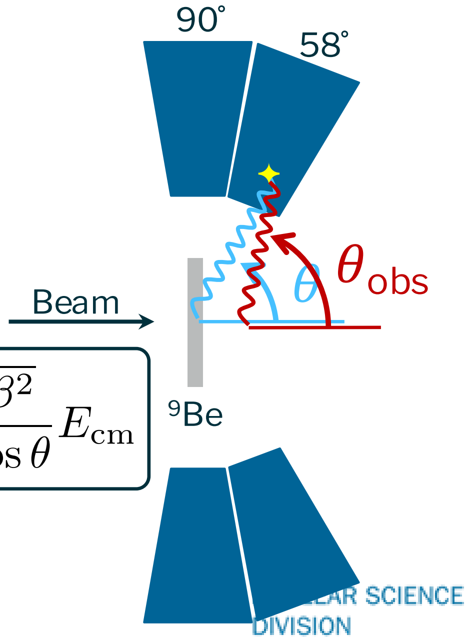

Example: ^{70}Fe

- States in ^{70}Fe were populated in -1p reaction from ^{71}Co
- Gamma-rays detected with GRETINA at the S800
- The high-resolution spectra enabled something odd to be noticed – the centroid of the 2+ state for two different rings of detectors was different for a mid-target Doppler correction
  - Characteristic of a lifetime effect

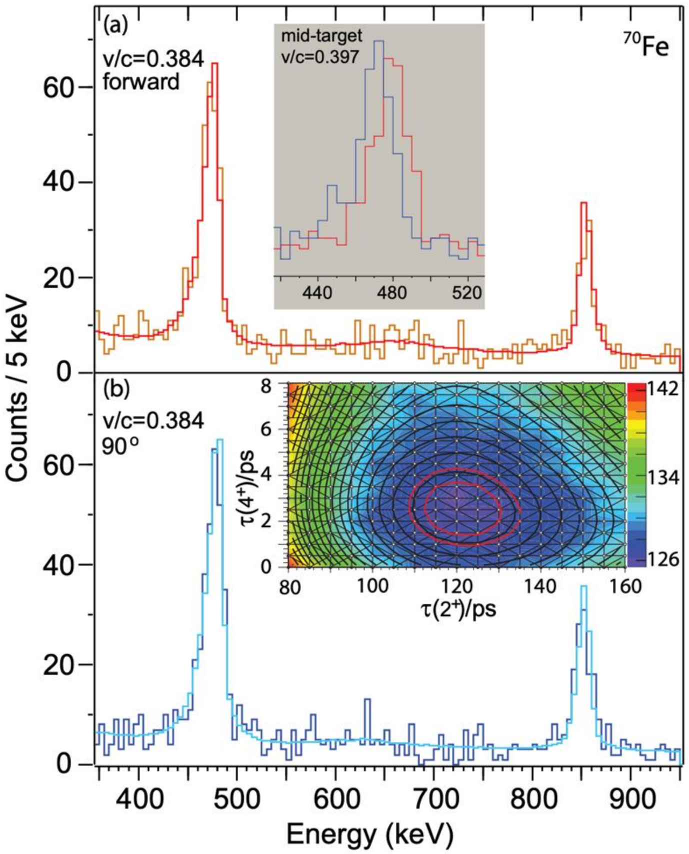

A. Gade *et al.*, Phys. Rev. C **99**, 011301 (2019).

BERKELEY LAB

Example: ^{70}Fe

- States in ^{70}Fe were populated in -1p reaction from ^{71}Co
- Gamma-rays detected with GRETINA at the S800
- The high-resolution spectra enabled something odd to be noticed – the centroid of the 2+ state for two different rings of detectors was different for a mid-target Doppler correction
  - Characteristic of a lifetime effect
  - Fit with simulated spectra enabled overall minimization of the lifetime of the observed 2+ and 4+ states

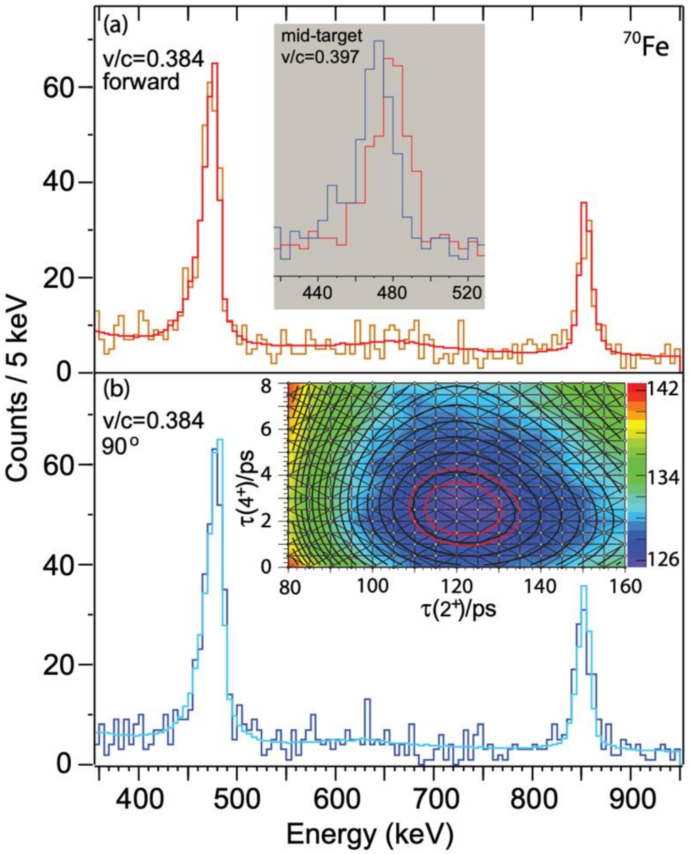

A. Gade *et al.*, Phys. Rev. C **99**, 011301 (2019).

BERKELEY LAB

Angular Distributions and Linear Polarization

- Angular distribution of a gamma-ray depends on the values of m_i and m_f

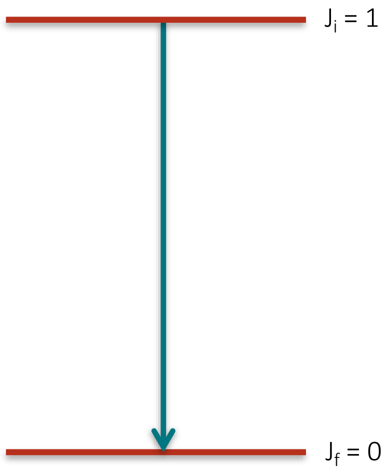

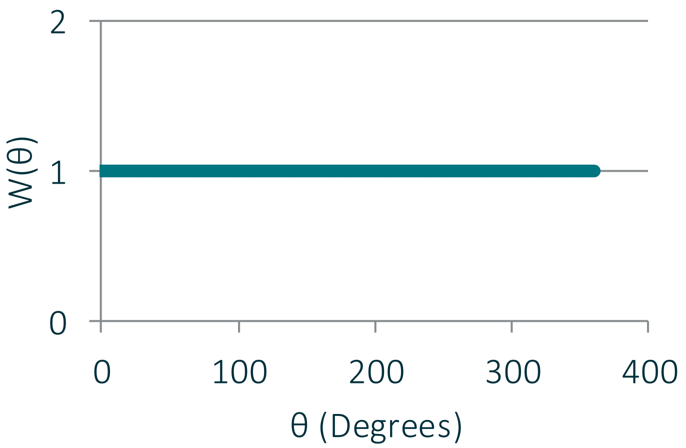

Angular Distributions and Linear Polarization

- Angular distribution of a gamma-ray depends on the values of m_i and m_f

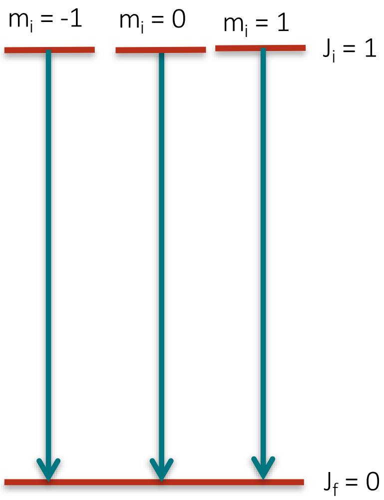

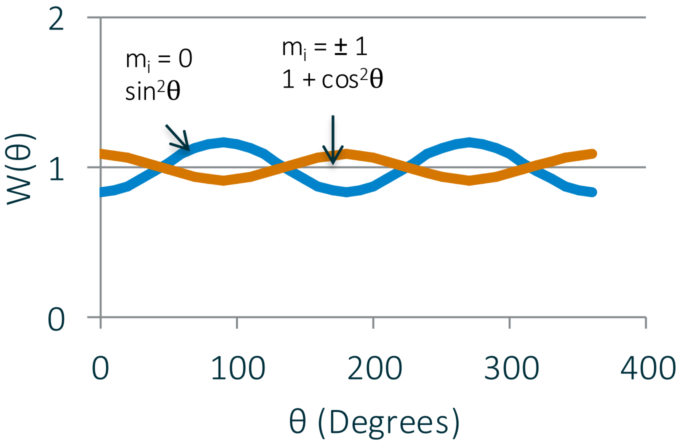

BERKELEY LAB

NUCLEAR SCIENCE DIVISION

Angular Distributions and Linear Polarization

- If we produce unequal populations $p(m_i)$ angular distributions $W(\theta)$ will be non-constant
- This condition can be created in nuclear reactions, where the populations with respect to the reaction plane are unequal
- Another way - Observation of a previous radiation selects an unequal mixture of populations $p(m_i)$

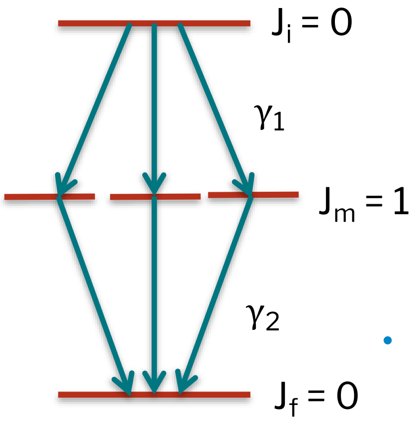

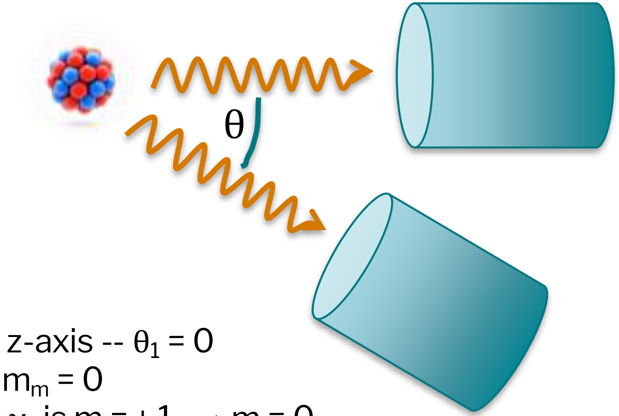

- First gamma defines z-axis -- $\theta_1 = 0$
  - $p(m_m) = 0$ for $m_m = 0$
- Distribution of γ_2 relative to γ_1 is $m = \pm 1 \longrightarrow m = 0$
  - $W(\theta) \rightarrow 1 + \cos^2\theta$

Angular Distributions and Linear Polarization

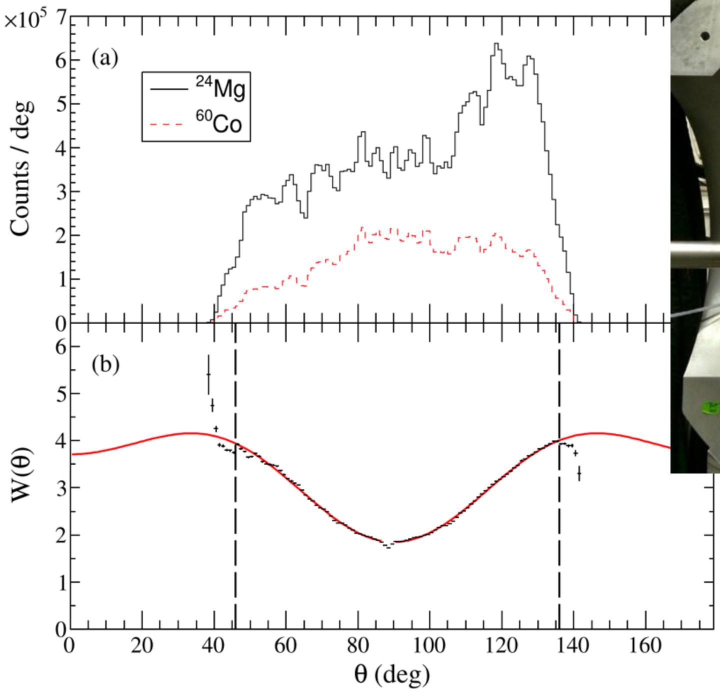

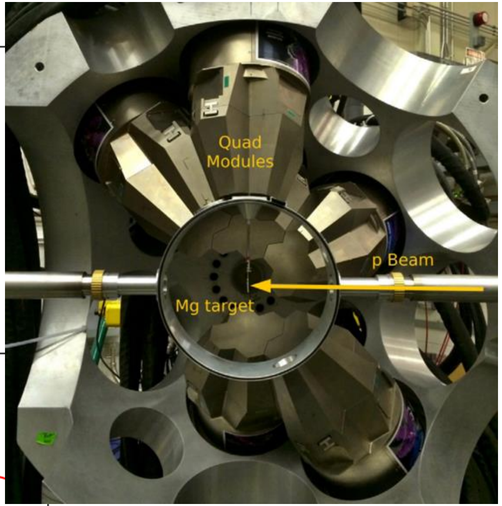

- ^{24}Mg(p,p') performed at 2.45 MeV proton energy produces very large alignment in the 2^+ state, with very strong hindrance of the m= ± 2 magnetic substates, and no feeding from above

C. Morse *et al.*, Nucl. Instrum. Methods Phys. Res. A **1025**, 166155 (2022).

Angular Distributions and **Linear Polarization**

- Gammas emitted from aligned states are also linear polarized, with the degree of polarization connected to the initial alignment
- Compton scattering, expressed through the Klein-Nishina formula, is sensitive to linear polarization

$$\frac{d\sigma}{d\Omega}(\psi,\chi) = \frac{1}{2} r_e^2 \left(\frac{E'_\gamma}{E_\gamma}\right)^2 \left[\frac{E'_\gamma}{E_\gamma} + \frac{E_\gamma}{E'_\gamma} - 2\sin^2\psi\cos^2\chi\right]$$

Angle between electric field vector of photon and the Compton scattering plane

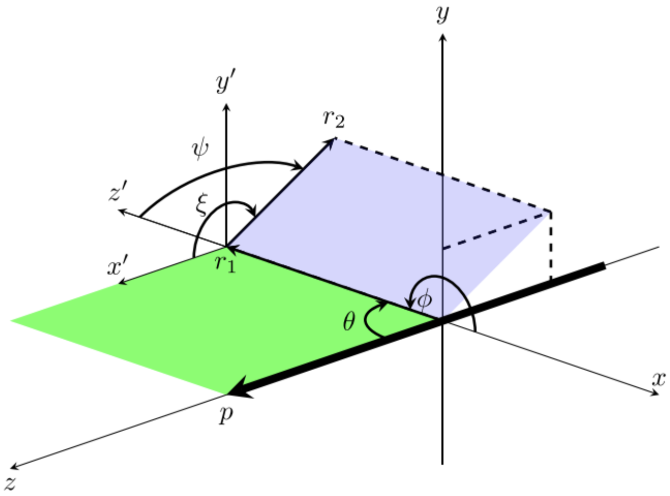

- More convenient to reformulate in terms of the distribution of the angle between the alignment plane and the Compton scattering plane, and integrate over our detection angles

$$W_c(\theta,\psi,\xi) = W(\theta)\frac{d\sigma}{d\Omega}(\psi)\left[1 - \frac{1}{2}\Sigma(\psi)P(\theta)\cos 2\xi\right]$$

$$W_c(\xi) = b(1 - A_0\cos 2\xi),$$

Angular Distributions and **Linear Polarization**

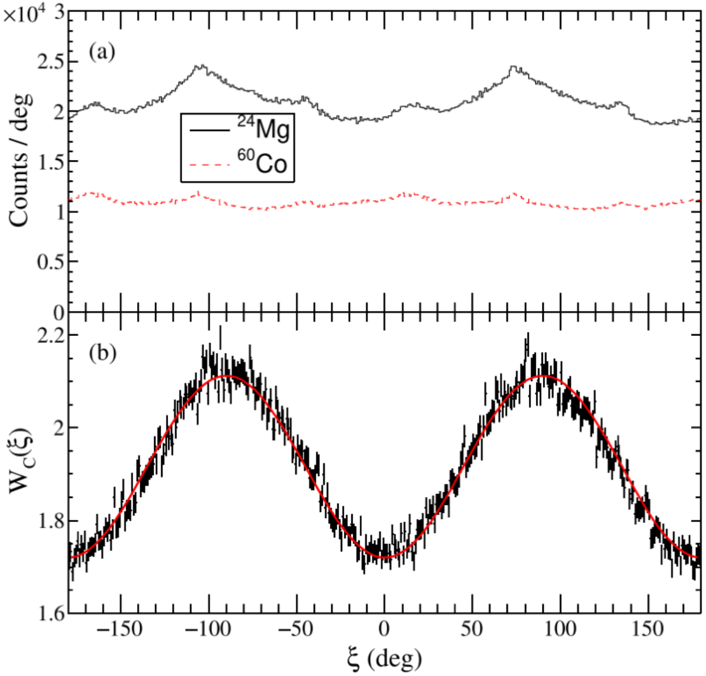

- Tracking arrays are **uniquely suited** for measurement of linear polarization – we measure (and order) Compton scattering interaction points across all scattering angles

Low-Energy Enhancement of the Gamma-Ray Strength Function

- The low-energy enhancement (LEE, or up-bend) in the gamma-ray strength function has been observed in many spherical / near-spherical nuclei (e.g. ^{56}Fe), but the origin of this enhancement or even it's nature is an open question
- The radiation has been experimentally shown to be dipole, but the electric/magnetic character is undetermined and theories provide contradictory predictions

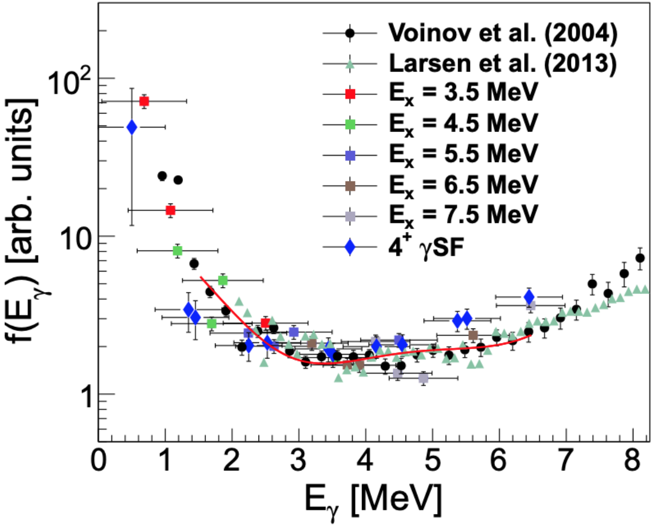

- A 2018 experiment led by LBNL attempted to measure the linear polarization of the LEE using GRETINA at ATLAS with the $^{56}Fe(p,p')$ reaction, but statistics were insufficient for a firm determination

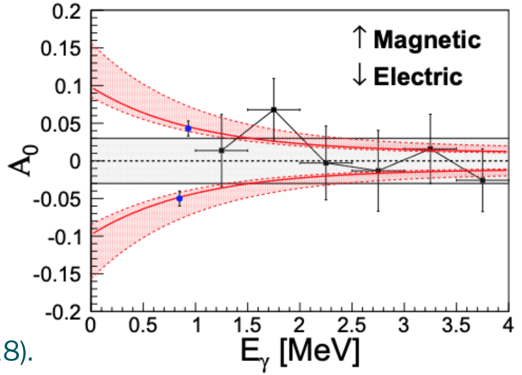

Jones *et al.*, PRC **97**, 024327 (2018).

Low-Energy Enhancement of the Gamma-Ray Strength Function

- The low-energy enhancement (LEE, or up-bend) in the gamma-ray strength function has been observed in many spherical / near-spherical nuclei (e.g. ^{56}Fe), but the origin of this enhancement or even it's nature is an open question
- The radiation has been experimentally shown to be dipole, but the electric/magnetic character is undetermined and theories provide contradictory predictions -- we gave now measured linear polarization confirming magnetic character

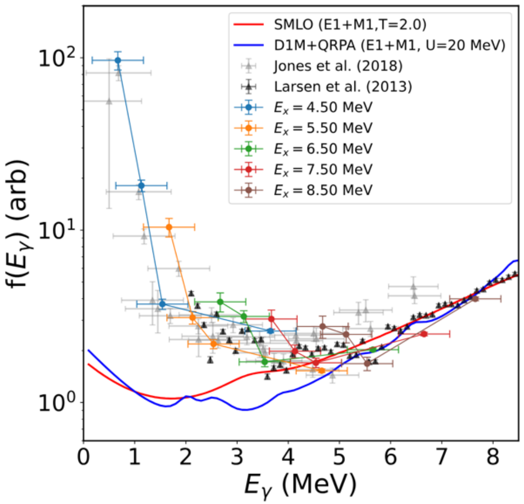

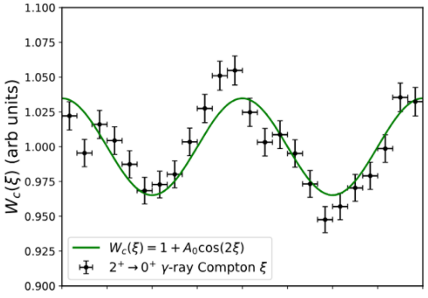

Polarization of $2^+ \to 0^+$

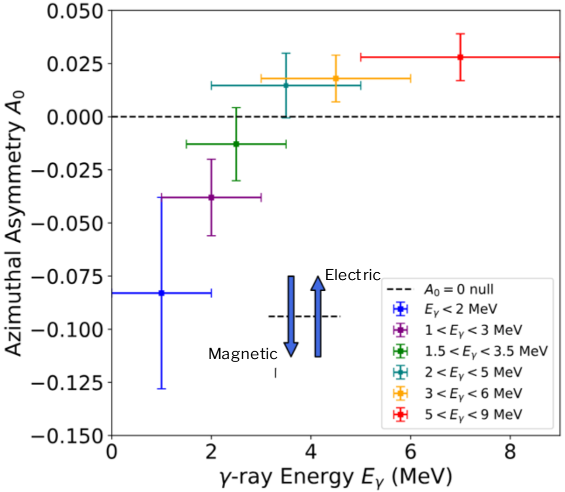

Discussion

- The performance of gamma-ray tracking detectors is very good, but the achieved position resolution is still worse than the theoretical limit – do you have any ideas why this might be?
- Where would you focus/what would you try to improve the P/T of a tracking array?

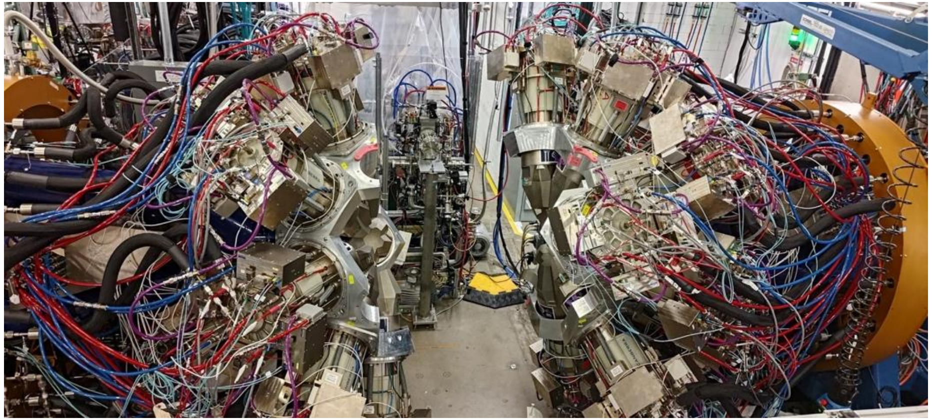

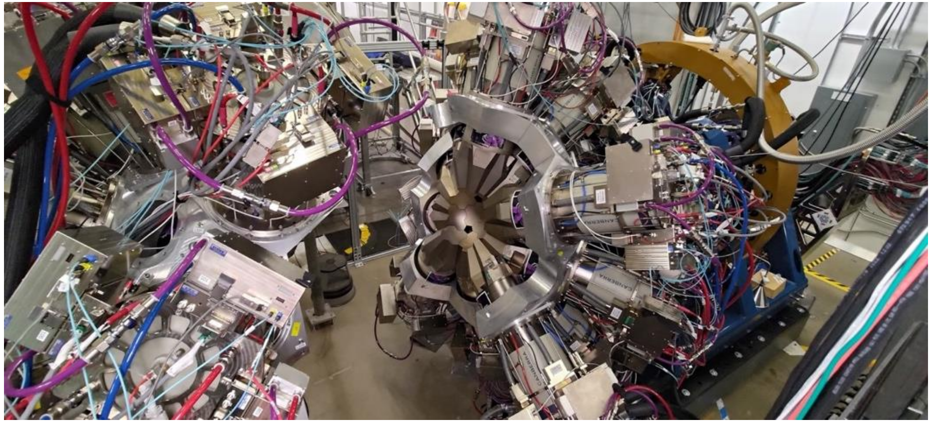

Questions?

Proton Density Bubble in ^{34}Si

- ^{34}Si was considered a candidate for a ”bubble” nucleus, with a deficit of proton density in the center region as compared to the neighbouring ^{36}S
- ^{34}Si(-1p)^{33}Al knockout reaction performed at NSCL (MSU) to probe occupancy of the proton $s_{1/2}$ orbital
- Goal → spectroscopic factor for knockout from $2s_{1/2}$

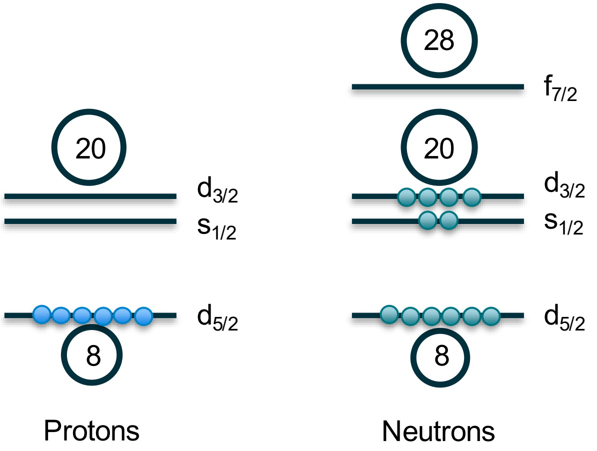

A. Mutschler *et al.*, Nature Physics **13**, 152 (2016).

Proton Density Bubble in ^{34}Si

- ^{34}Si(-1p)^{33}Al knockout reaction on ^{9}Be target using the S800 spectrometer and GRETINA

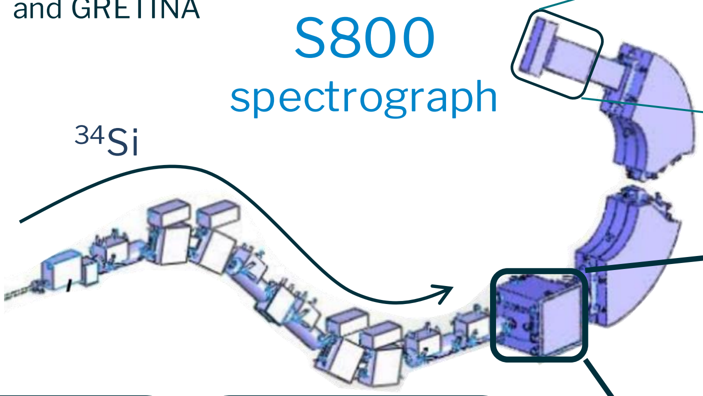

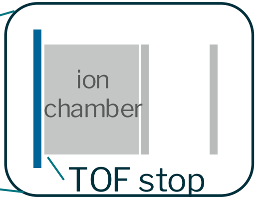

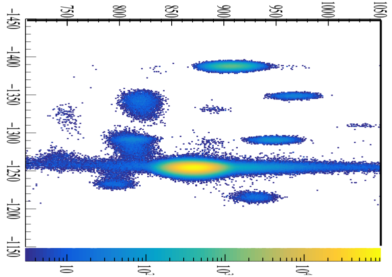

GRETINA gamma-ray spectrometer

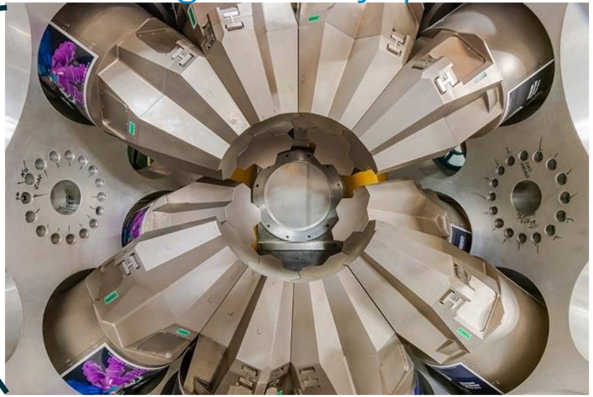

https://people.nscl.msu.edu/~noji/gret_12det

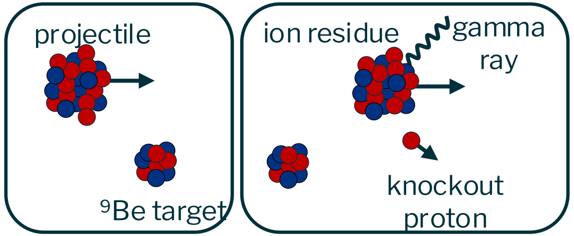

Proton Density Bubble in ^{34}Si

- $^{34}Si(-1p)^{33}Al$ knockout reaction on ^{9}Be target using the S800 spectrometer and GRETINA

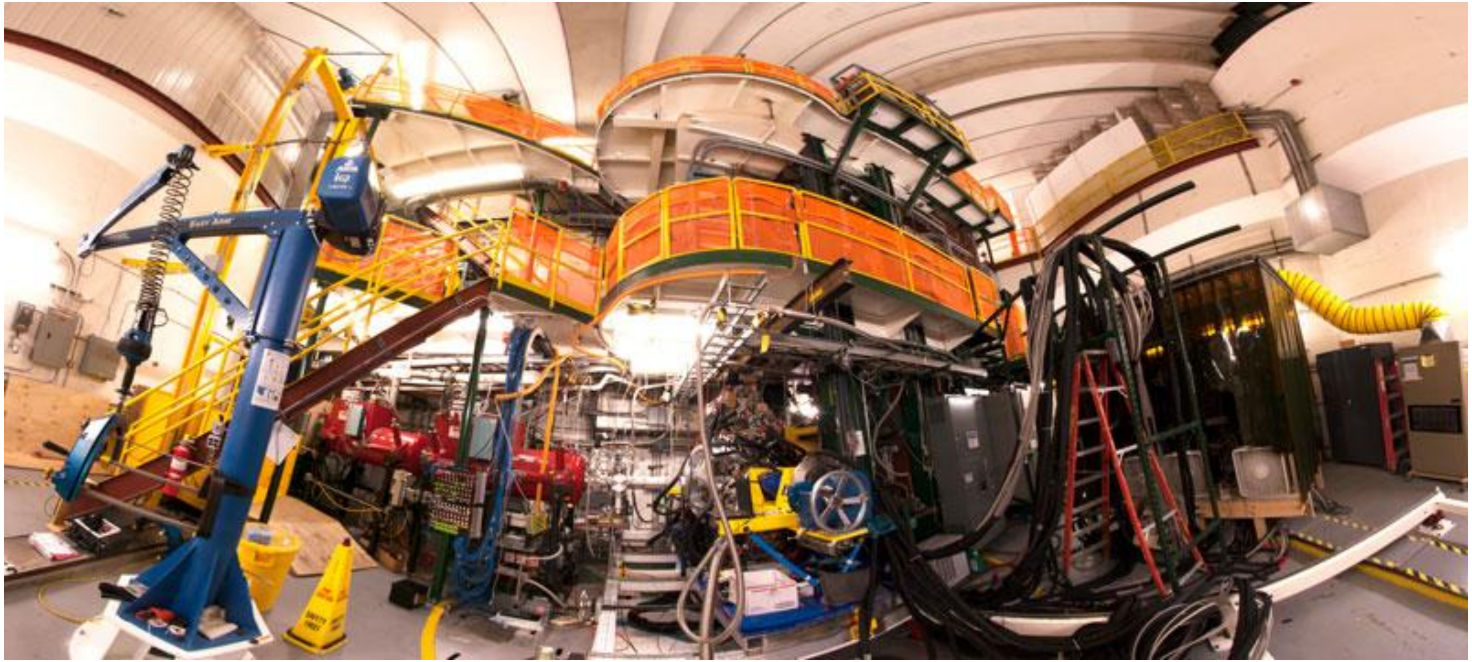

Proton Density Bubble in ^{34}Si

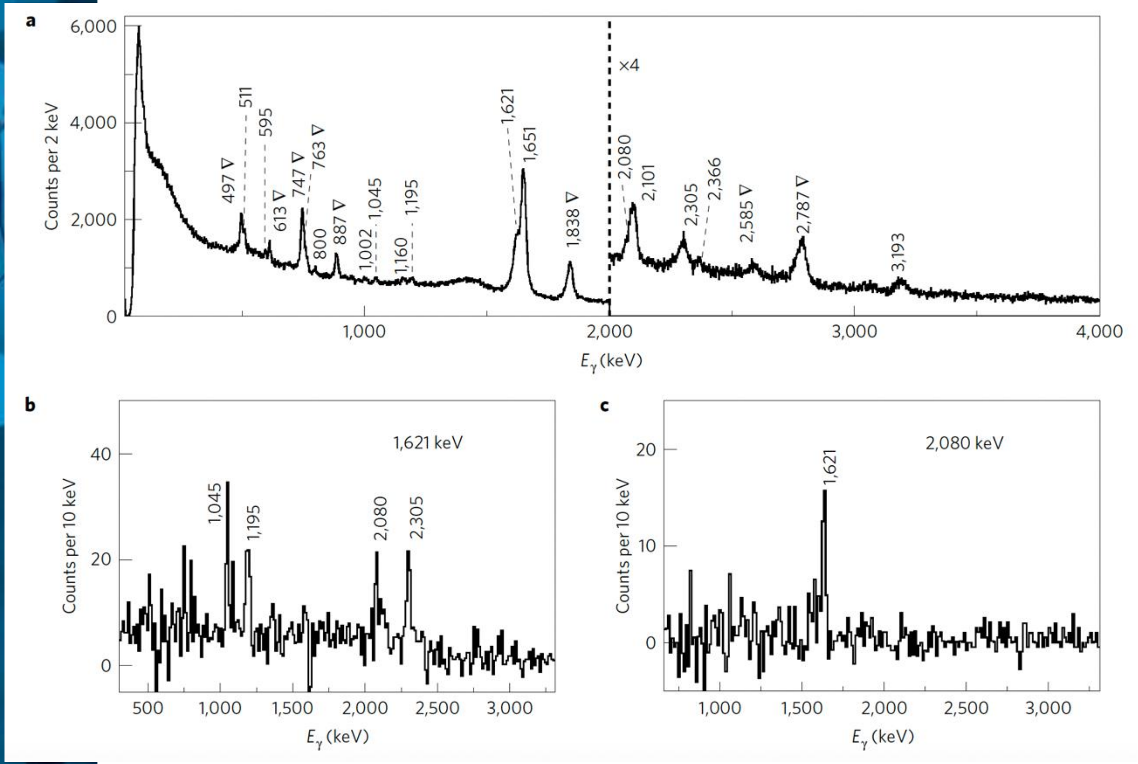

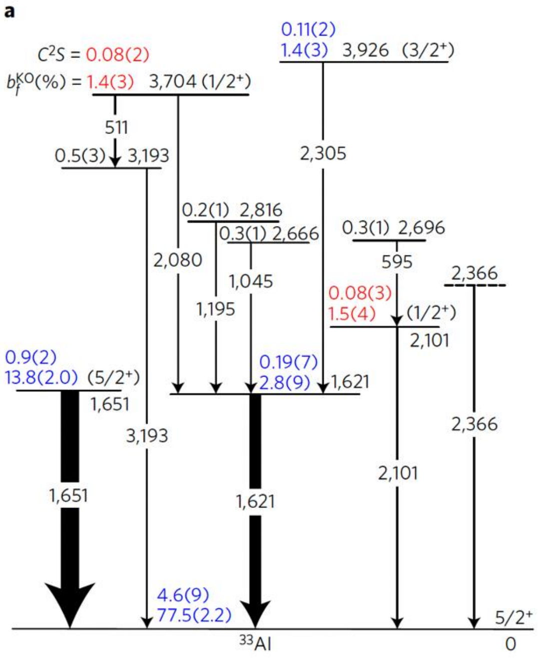

A. Mutschler *et al.*, Nature Physics **13**, 152 (2016).

Proton Density Bubble in ^{34}Si

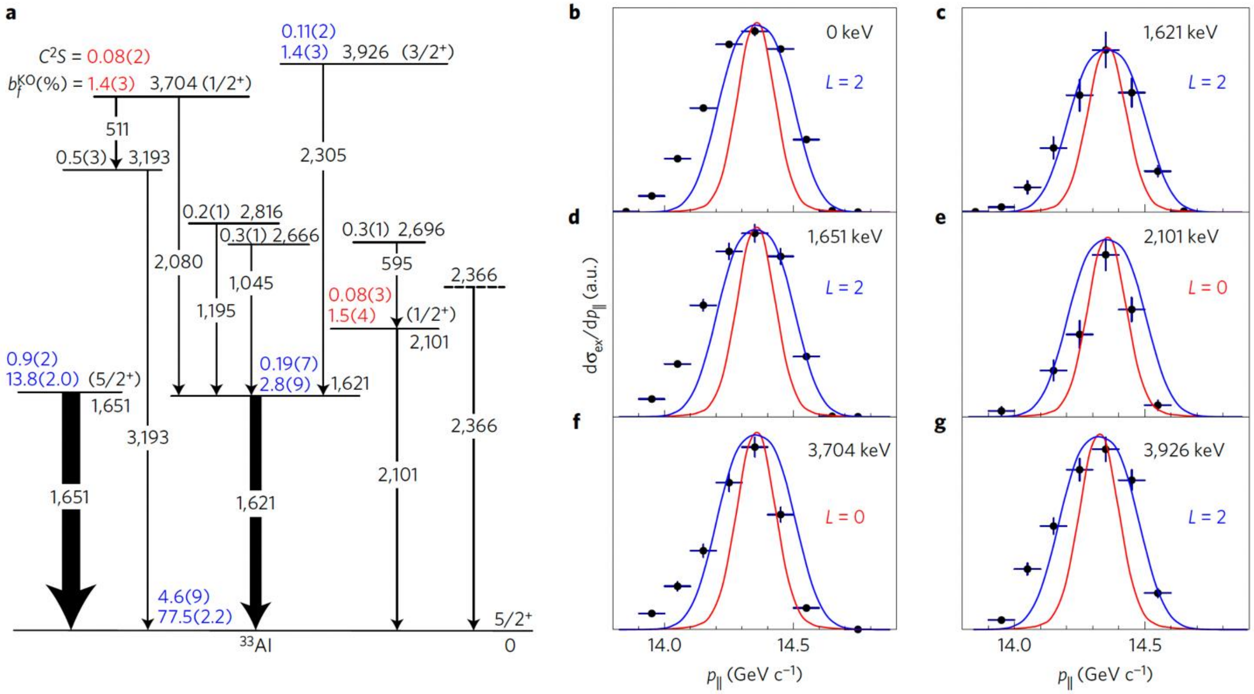

A. Mutschler *et al.*, Nature Physics **13**, 152 (2016).

Proton Density Bubble in ^{34}Si

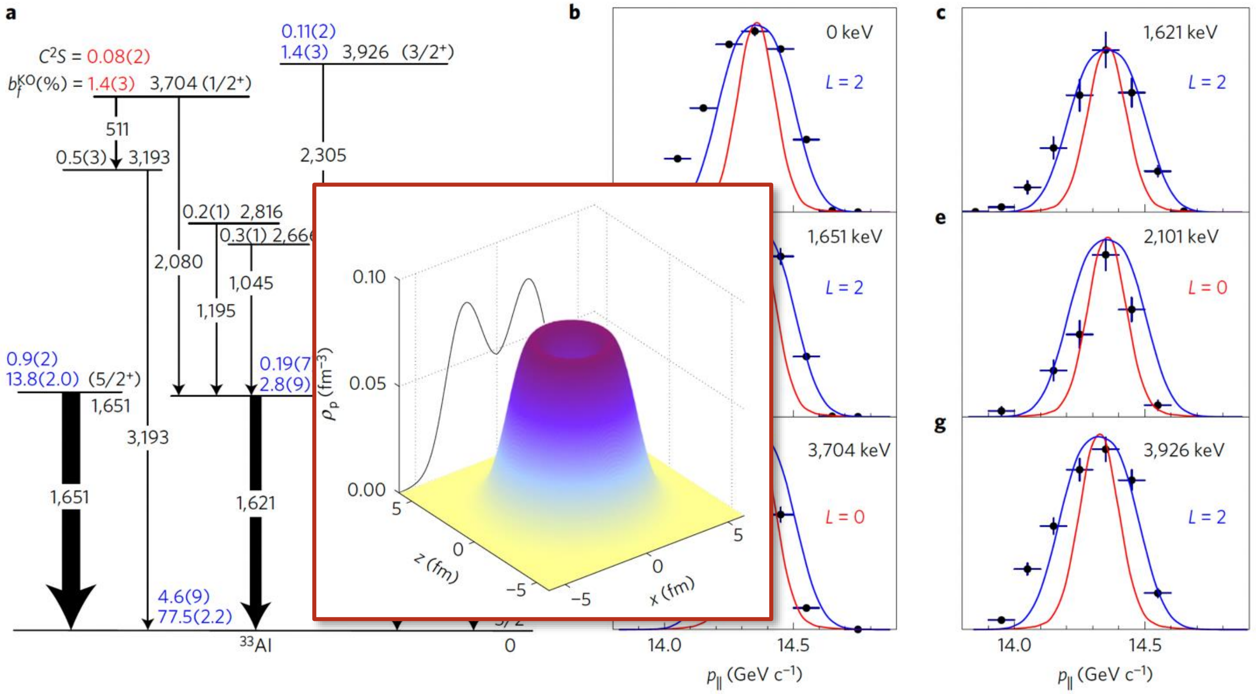

A. Mutschler *et al.*, Nature Physics **13**, 152 (2016).

BERKELEY LAB

NUCLEAR SCIENCE DIVISION

Example: Pear Shaped Nuclei

The case of ^{224}Ra

- Beyond quadrupole deformation, octupole collectivity is expected where excitations with ΔJ, ΔL = 3 are possible (enhanced near octupole 'magic numbers' = 34, 56, 88, 134)
- ^{222,224}Ra lie near Z=88 and N=134 ⇒
- Macroscopically, octupole correlations lead to a "pear-shaped" nucleus, breaking reflection symmetry
- Signatures for octupole?
  - Enhanced E1 transitions
  - Odd-even staggering, negative parity states at low E
  - Large E3 strength ⇒ B(E3: 0+ → 3-)

$$\pi\left(f_{7/2} \rightarrow i_{13/2}\right) \quad \nu\left(g_{9/2} \rightarrow j_{15/2}\right)$$

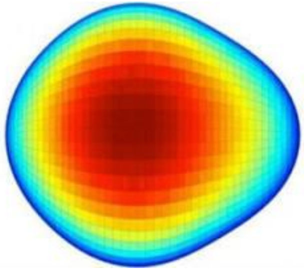

L. P. Gaffney *et al.*, Nature **497**, 199 (2013).

Coulex at REX-ISOLDE with MINIBALL

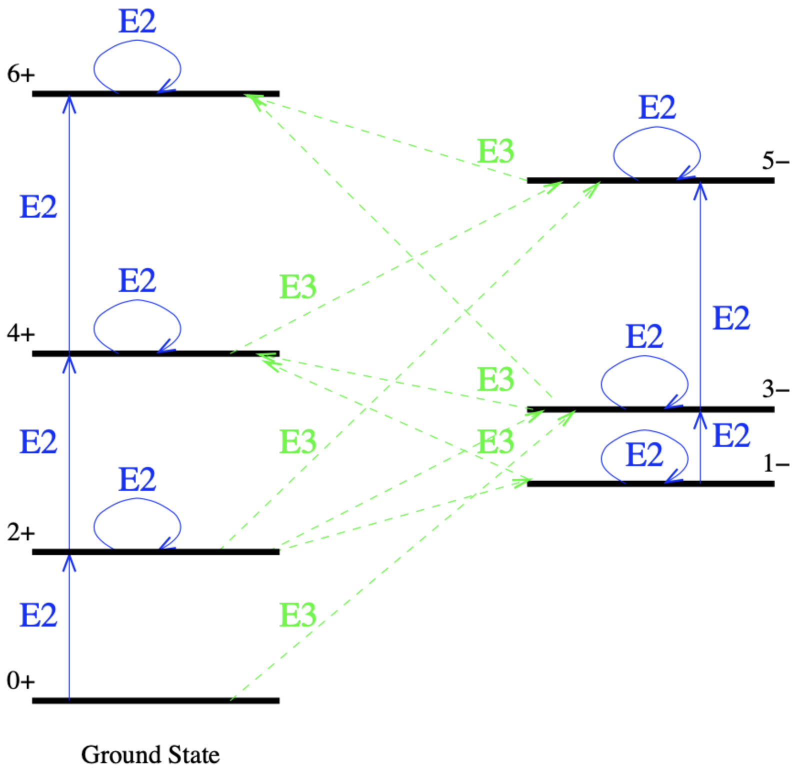

L. P. Gaffney *et al.* Nature 497, 199 (2013).

Coulex at REX-ISOLDE with MINIBALL

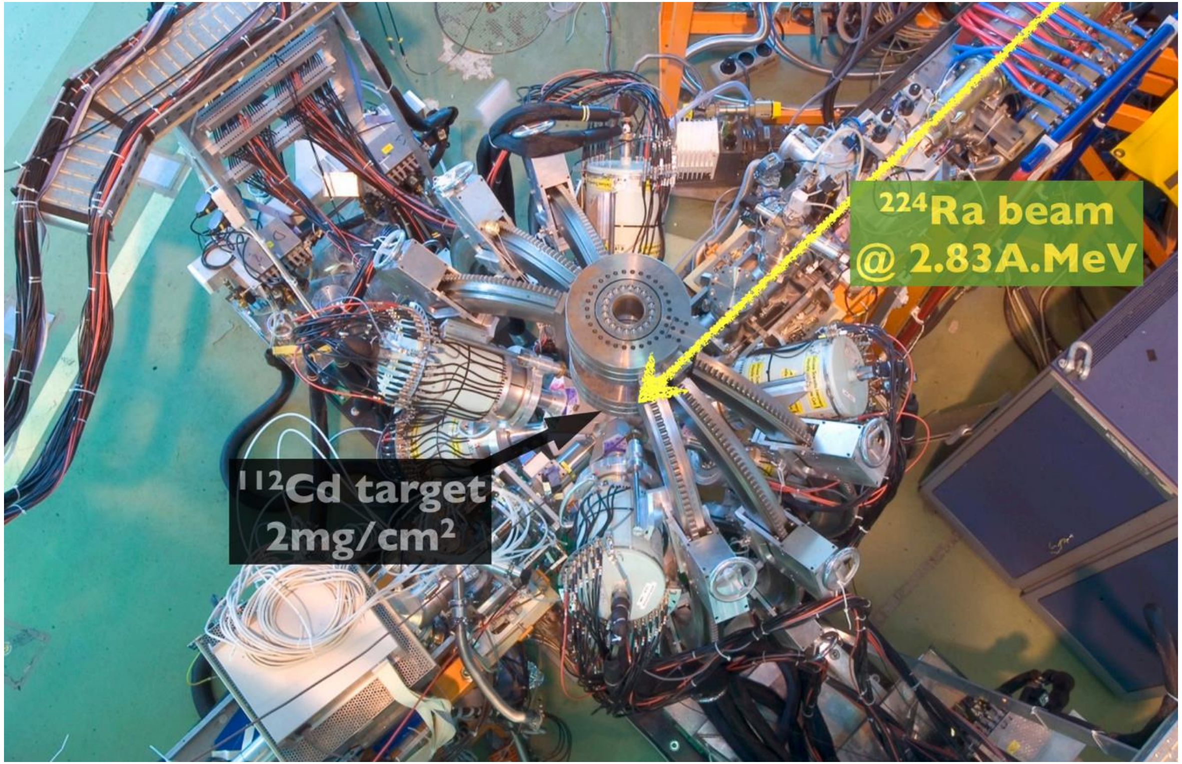

L. P. Gaffney *et al*., Nature **497**, 199 (2013).

Coulex at REX-ISOLDE with MINIBALL

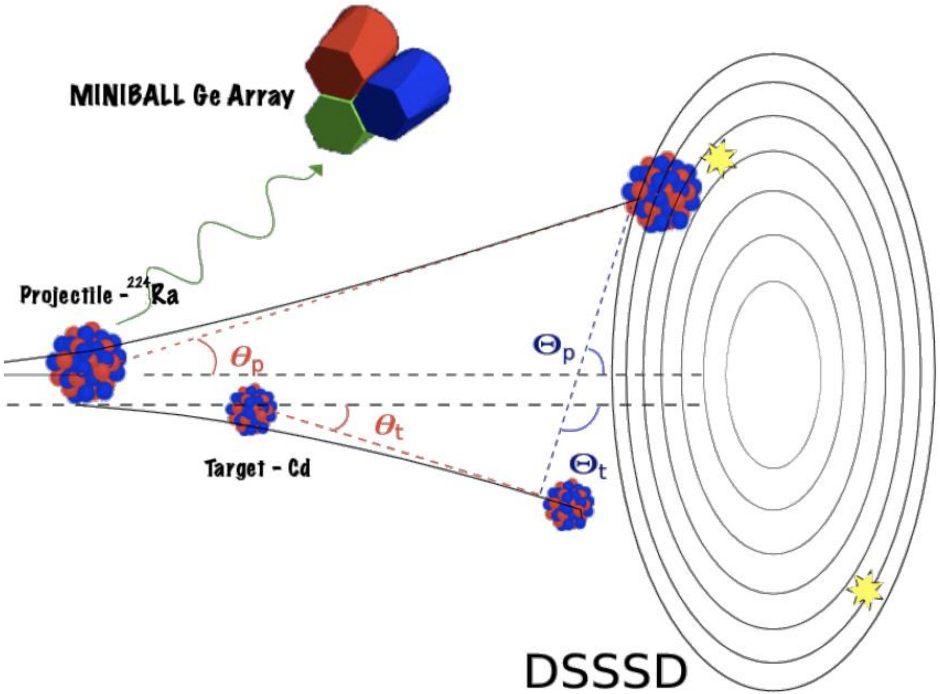

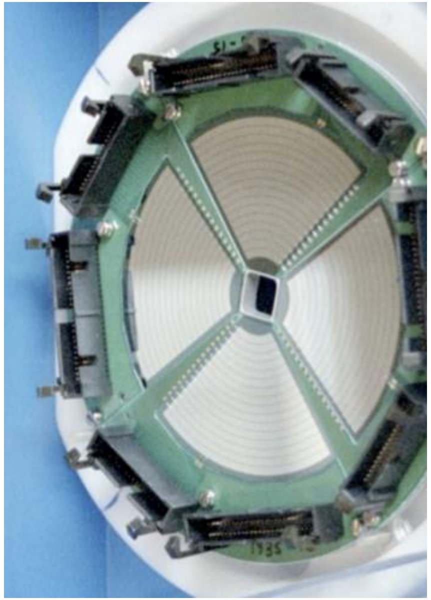

L. P. Gaffney *et al*., Nature **497**, 199 (2013).

Coulex at REX-ISOLDE with MINIBALL

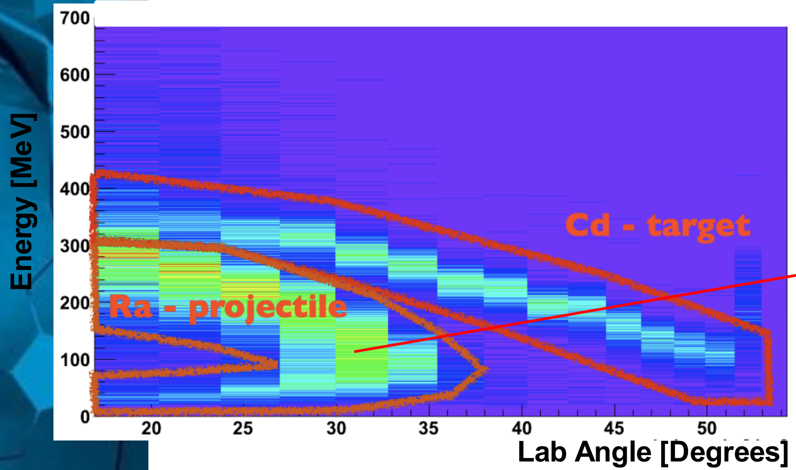

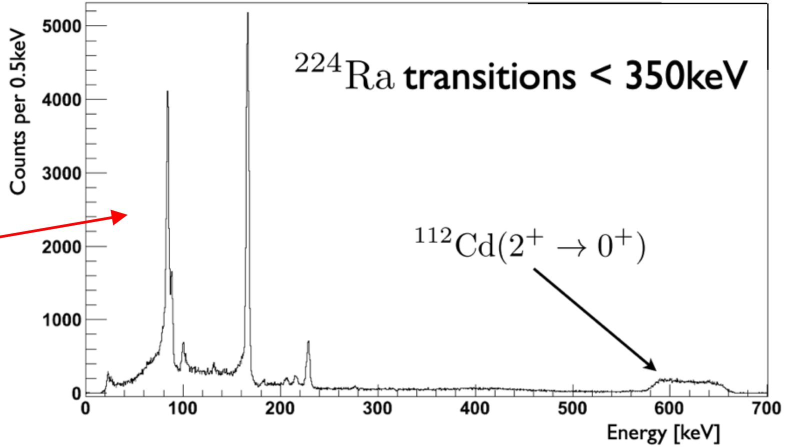

L. P. Gaffney *et al.* Nature 497, 199 (2013).

Coulex at REX-ISOLDE with MINIBALL

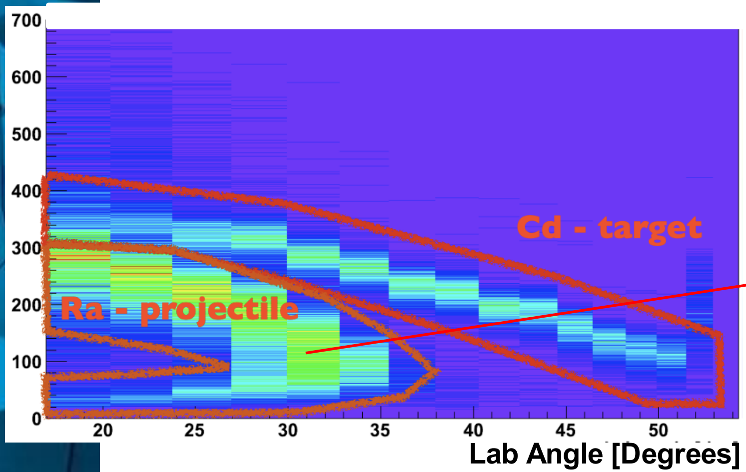

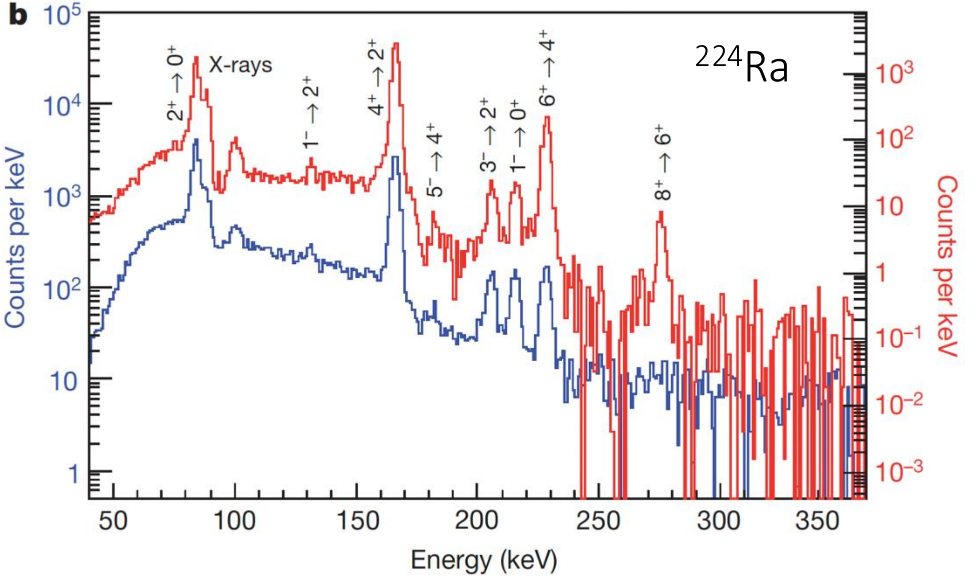

L. P. Gaffney *et al.* Nature 497, 199 (2013).

Example: Pear Shaped Nuclei

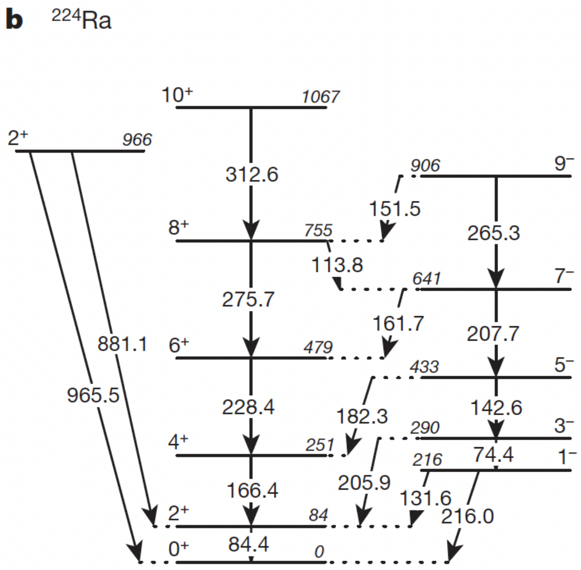

^{224}Ra

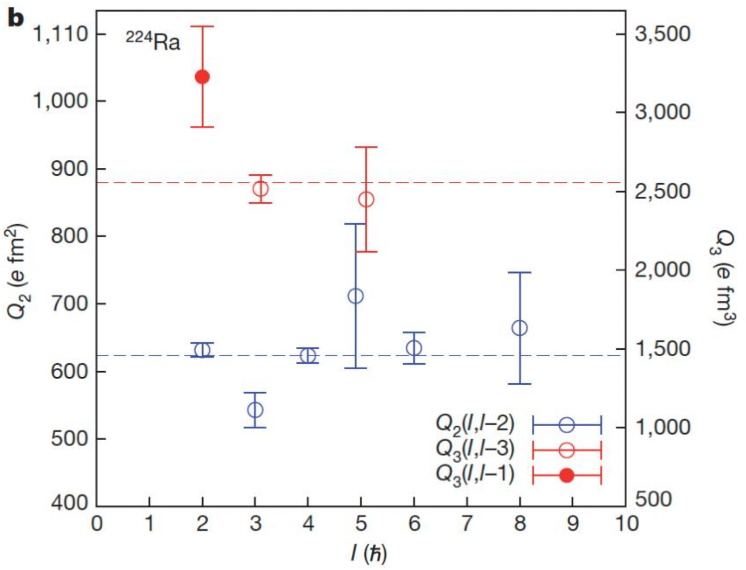

$$\langle I' || \mathrm{E}\lambda || I \rangle = \sqrt{(2I'+1)(2\lambda+1)/16\pi}\,(I'0\lambda0|I0)\,Q_\lambda$$

L. P. Gaffney *et al.*, Nature **497**, 199 (2013).

Example: Pear Shaped Nuclei

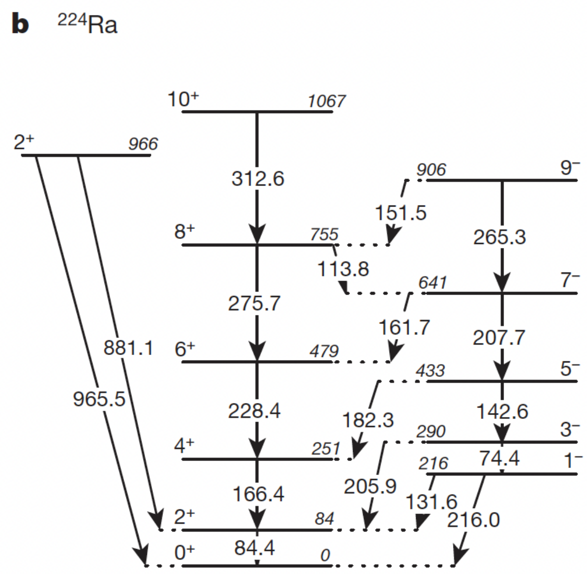

^{224}Ra

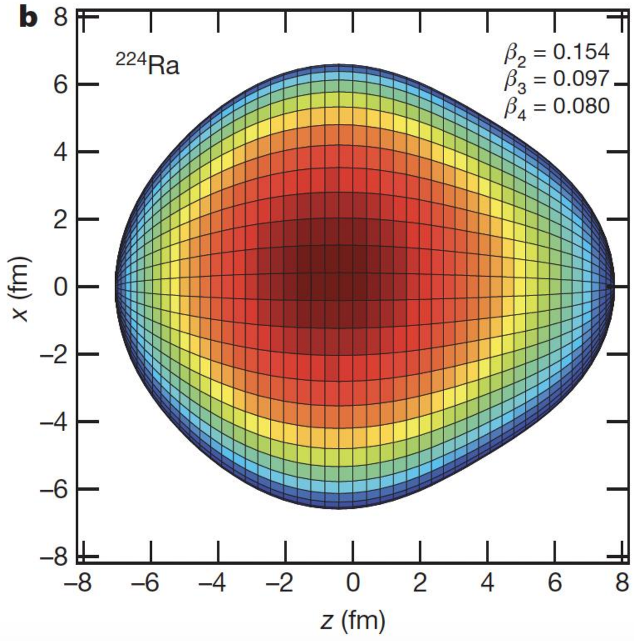

L. P. Gaffney *et al.* Nature 497, 199 (2013).

Lifetimes and transition probabilities

Transition probability for gamma-decay relates strongly to specific nuclear matrix elements → provide a stringent test of theoretical wavefunctions

Consider the case of the first 2+ states in even-even nuclei

$$\tau_\gamma = 40.81 \times 10^{13} E^{-5} [B(E2)\uparrow / \mathrm{e}^2\mathrm{b}^2]^{-1}$$

$$B(E2 : J_i \rightarrow J_f) = \frac{1}{2J_i + 1} \langle \psi_f || E2 || \psi_i \rangle^2$$

Lifetimes are of order ps --> how do we measure these lifetimes?

Recoil-distance (plunger) method

The lifetime of excited states in the range of 10-100s of ps can be measured by populating the state via Coulomb excitation or knock-out reactions and observing the Doppler-shift of the decay gamma-ray.

$$E_\gamma = E_\gamma^0 \frac{\sqrt{1-\beta^2}}{1-\beta\cos\theta}$$

In green region, nuclei are moving with velocity β, we can correct exactly to recover E_γ^0

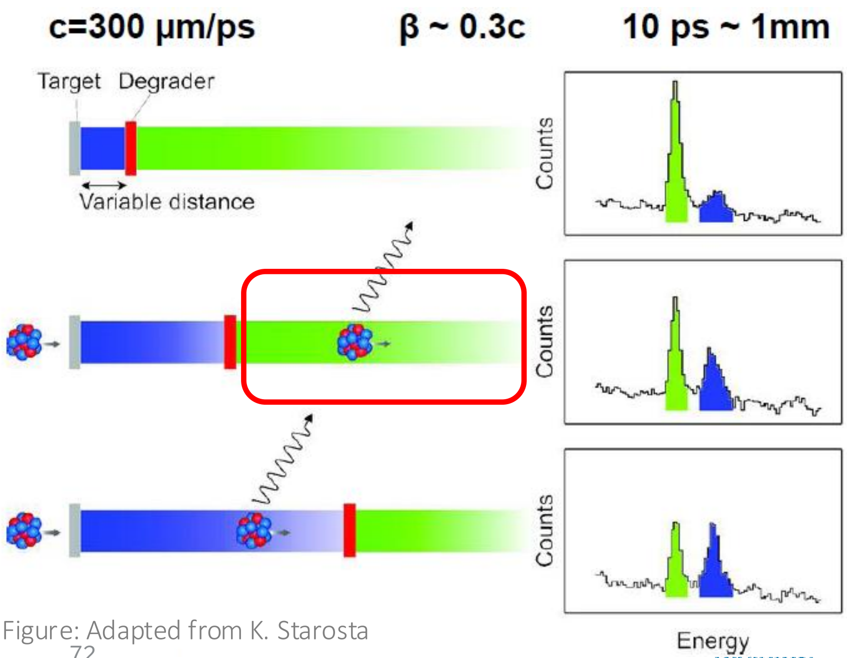

Figure: Adapted from K. Starosta

Recoil-distance (plunger) method

The lifetime of excited states in the range of 10-100s of ps can be measured by populating the state via Coulomb excitation or knock-out reactions and observing the Doppler-shift of the decay gamma-ray.

$$E_\gamma = E_\gamma^0 \frac{\sqrt{1-\beta^2}}{1-\beta\cos\theta}$$

In green region, nuclei are moving with velocity β, we can correct exactly to recover E_γ^0

In blue region, we have (β+$\Delta\beta$). When we Doppler correct with assuming β we are slightly wrong and correct to > E_γ^0

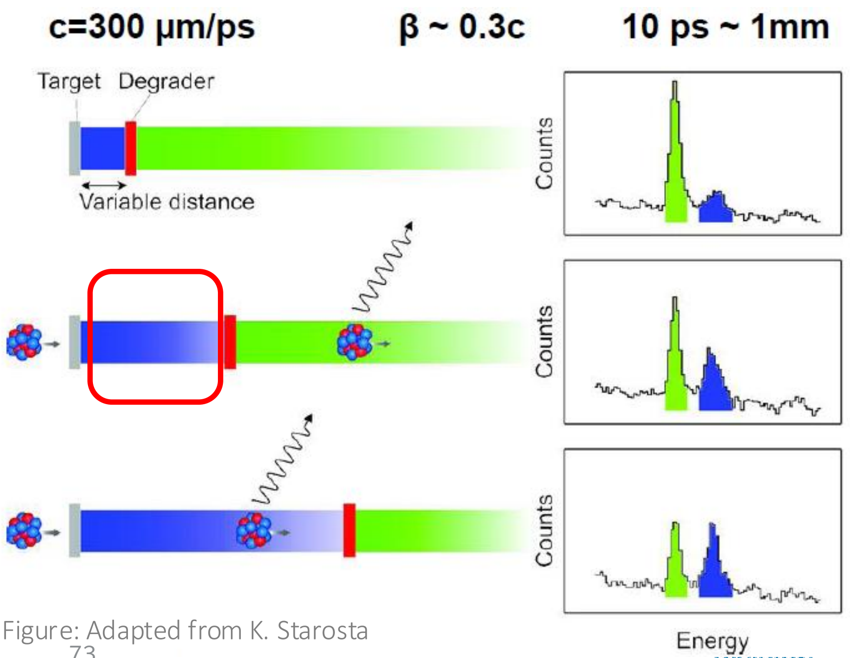

Figure: Adapted from K. Starosta

BERKELEY LAB

Example: Lifetimes in $^{72,74}Kr$

- The even-even neutron-deficient isotopes are a region of the nuclear chart in which the ground-state deformation changes from prolate (rugby ball) to oblate (pancake) approaching $^{72}Kr_{36}$
- Goal was to explore the evolution of collectivity toward ^{72}Kr by measuring lifetimes of the yrast 2+ and 4+ states to access the corresponding B(E2) values
- Populated excited states in $^{72,74}Kr$ using -2n removal and inelastic scattering with ^{74}Kr beam on ^{9}Be target
- Performed at NSCL (MSU) using GRETINA around the target position and the S800 to identify reaction residues

H. Iwasaki *et al.*, Phys. Rev. Lett. 112, 142502 (2014).

Example: Lifetimes in ^{72,74}Kr

- Used the TRIPLEX plunger for lifetime sensitivity
- Enables two distances to be probed at once to better constrain lifetimes

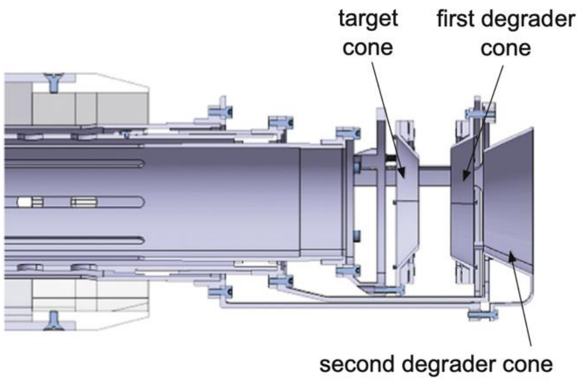

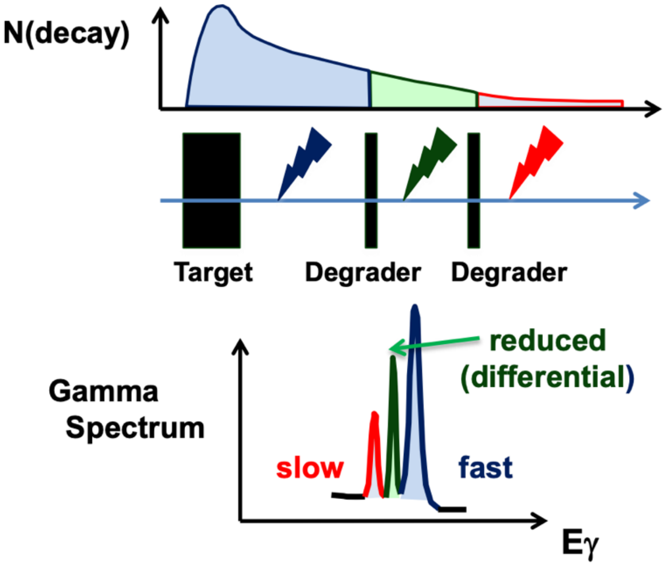

H. Iwasaki *et al.*, Phys. Rev. Lett. 112, 142502 (2014).

Lifetimes in ^{72,74}Kr

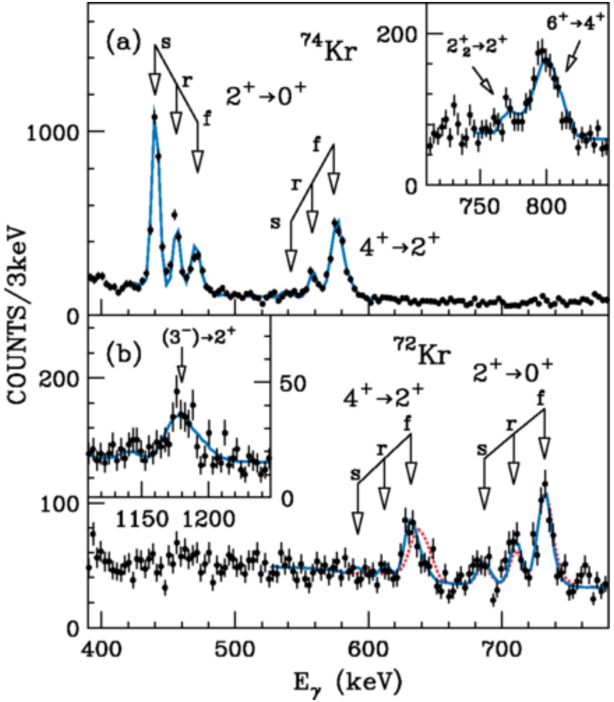

H. Iwasaki *et al.*, Phys. Rev. Lett. **112**, 142502 (2014).

- Lifetimes were related to the reduced transition probabilities B(E2) and compared with theory predictions
- Here, the irregular behaviour for the 4+ and 2+ states suggest a rapid shape evolution in ^{72}Kr with a transition to prolate character at higher spins

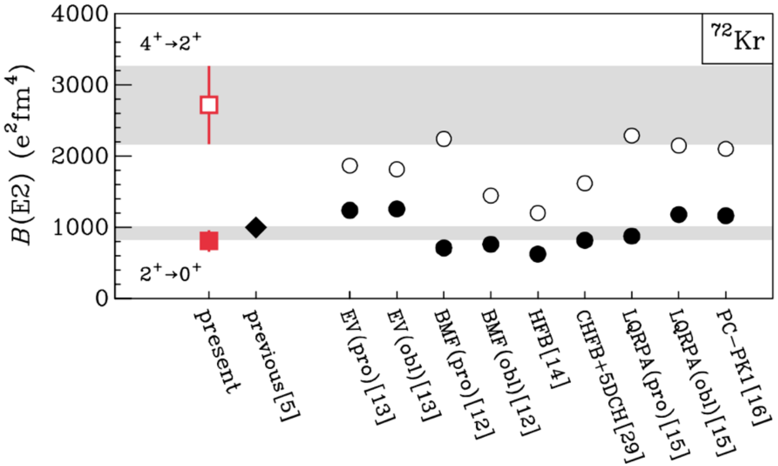

BERKELEY LAB

NUCLEAR SCIENCE DIVISION